One engram two readouts: stimulus dynamics switch a learned behavior in *Drosophila*

Mehrab N Modi[a], Adithya Rajagopalan[a,b], Hervé Rouault[a,c], Yoshinori Aso[a], Glenn C Turner*[a]

a HHMI Janelia Research Campus, 19700 Helix Drive, Ashburn VA, 20147, USA
b The Solomon H. Snyder Department of Neuroscience, Johns Hopkins University School of Medicine, Baltimore, MD 21205, USA
c Aix-Marseille Univ, Université de Toulon, CNRS, CPT (UMR 7332), Turing Centre for Living systems, Marseille, France

Mehrab N Modi - modim@janelia.hhmi.org
Adithya Rajagopalan - rajagopalana@janelia.hhmi.org
Hervé Rouault - herve.rouault@univ-amu.fr
Yoshinori Aso - asoy@janelia.hhmi.org
Glenn C Turner - turnerg@janelia.hhmi.org*

Keywords: Synaptic plasticity; Discrimination; Generalization; Memory Template

Summary:

Memory guides the choices an animal makes across widely varying conditions in dynamic environments. Consequently, the most adaptive choice depends on the options available. How can the same memory support optimal behavior across different sets of options? We address this using olfactory learning in Drosophila. Even when we restrict an odor-punishment association to a single set of synapses using optogenetics, we find that flies still show choice behavior that depends on the options it encounters. Here we show that how odors are presented to the animal influences memory recall itself. Presenting two similar odors in sequence enabled flies to not only discriminate them behaviorally but also at the level of neural activity. However, when the same odors were encountered as solitary stimuli, no such differences were detectable. These results show that memory recall is not simply a comparison between a stimulus and a learned template, but can be adaptively modulated by stimulus dynamics.

Introduction:

Animals routinely encounter competing options and must select the most beneficial behavior to execute and survive in complex environments. Making choices is thought to consist of multiple cognitive processes, from representations of the choice stimuli (Miura, Mainen, and Uchida 2012; Honegger, Campbell, and Turner 2011), to subjective evaluations of the alternatives (Hunt et al. 2012; Seger 2008). Remembered experience then updates the perceived values of those cues. This is how memories are integrated into other computations to drive choice behavior (Hare et al. 2011). However, the most adaptive behavioral response is to choose the stimulus of highest value to the animal. Hence, the response to a given stimulus should depend on whether its remembered, subjective value is higher or lower than the available alternatives - the best choice among one set of options may be superseded by a different option when things change, and choice behavior should adjust accordingly. How do the choices available influence memory recall?

A classic example of how available options influence choice are discriminination and generalization tasks. Discrimination tasks typically require the animal to distinguish between one cue they have formed an association with, and a second, perceptually similar cue. Animals can perform such tasks very well, and their choice behavior is driven by the cue they were trained with. However, if the animal is instead presented with a choice between that perceptually similar cue and a distinct option, the subjective value of the trained cue is generalized to the similar one. Hence, the animal's choice behavior will be driven by the perceptually similar cue. Notably, the opposite choice behavior is required in the two settings. For example, an animal may learn that oranges are very rewarding, and so chooses oranges over grapefruit. However, if given a choice between grapefruit and a very different option, such as banana, they may generalize the association across citrus fruits and choose grapefruit. Despite the need to switch choices in these two situations, performance can be extremely high on both these types of tasks (Campbell et al. 2013; Xu and Südhof 2013), suggesting that the choices available have a strong impact on how an animal uses what it has learned. We used these two types of tasks to examine how choice influences memory retrieval, using olfactory conditioning in Drosophila.

In Drosophila, odor memory is thought to be stored in the output synapses of a population of ~2000 Kenyon cells (KCs) that are the intrinsic neurons of the mushroom body (MB) — a third order brain structure loosely analogous to piriform cortex in the mammalian brain. Different odors elicit sparse and largely decorrelated patterns of KC activity. During learning, these representations are thought to form a template of the learned odor stimulus by changing the weights of the KCs that represent the learned odor onto downstream neurons(Hopfield 1982; Shepard 1987; Tenenbaum and Griffiths 2001; Modi, Shuai, and Turner 2020). Odors with similar chemical structures tend to elicit activity in overlapping sets of KCs, and such correlated activity is predictive of flies' performance in a generalization task(Campbell et al. 2013). Circuit manipulations controlling the degree of overlap between response patterns directly showed that increasing overlap decreases discriminability(A. C. Lin et al. 2014). Overall these studies support the idea that stimulus specificity of memory in this circuit is based on a template

matching process, where a high match to the learned template supports generalization and low match drives discrimination.

How is the match to template read out by downstream circuitry? The typical MB Output Neurons (MBONs) are a set of ~30 neurons per hemisphere which have extensive dendritic trees that innervate the peduncle and lobes of the MB, where they integrate input from different subsets of KCs(Crittenden et al. 1998; Ito et al. 1998; Strausfeld, Sinakevitch, and Vilinsky 2003; H.-H. Lin et al. 2007; Tanaka, Tanimoto, and Ito 2008; Aso et al. 2009; Aso, Hattori, et al. 2014; Takemura et al. 2017; Li et al. 2020). Optogenetic stimulation experiments established that MBONs can elicit behavioral responses that resemble attraction or aversion to odor(Aso, Sitaraman, et al. 2014; Owald et al. 2015). The dendrites of different MBONs tile the length of the KC axon bundles in a series of 15 non-overlapping compartments(Tanaka, Tanimoto, and Ito 2008; Aso, Hattori, et al. 2014; Takemura et al. 2017; Li et al. 2020). Dopaminergic neurons (DANs) arborize in corresponding zones, matching up to the different MBONs to form a series of DAN-MBON modules(Aso, Hattori, et al. 2014). DANs convey information about reward or punishment to their target compartment, where they drive plasticity of KC>MBON synapses, thereby changing the mapping of odor identity to valence. This plasticity is typically synaptic depression; for example learning an odor-punishment association induces synaptic depression of the responding KCs onto MBONs that drive approach behavior(Séjourné et al. 2011; Hige, Aso, Modi, et al. 2015; Cohn, Morantte, and Ruta 2015; Perisse et al. 2016; Berry, Phan, and Davis 2018) but see also (Plaçais et al. 2013; Stahl et al. 2022).

Plasticity can be targeted to individual compartments using optogenetic stimulation of specific DANs in place of a physical reinforcer. Using optogenetic reinforcement revealed that learning in different compartments is governed by different plasticity properties(Hige, Aso, Modi, et al. 2015; Aso and Rubin 2016). Compartments vary in their threshold for memory induction, duration of memory retention, and susceptibility to disruption, amongst other features(Aso and Rubin 2016; Hige, Aso, Modi, et al. 2015; Huetteroth et al. 2015; König et al. 2017; Yamagata et al. 2015). This approach also revealed how overlap in the KC representations of two odors is reflected in the specificity of the synaptic changes that drive learning. KCs are cholinergic and excitatory to MBONs(Barnstedt et al. 2016), so when training drives synaptic depression of KCs activated by the the odor paired with reinforcement, MBON response to odors with partially overlapping KC activity patterns are also reduced (Hige, Aso, Modi, et al. 2015). The greater the overlap, the greater the reduction in the MBON response and the stronger the generalization of the original association. In this sense, MBON activity signals the extent of mismatch to the learned odor. However, this raises an important question in the context of choice-dependent recall. If the mismatch signal conveyed by MBON responses to an odor is identical irrespective of the choices presented to the animal, how can it drive the different choice behavior necessary to achieve high performance in both discrimination and generalization tasks?

In this study, we examined the odor specificity of learning in different MB compartments, using optogenetic reinforcement targeted to specific compartments. We used behavioral experiments to identify an MB compartment capable of supporting similar levels of performance for both hard discrimination and generalization. Surprisingly, functional imaging experiments that evaluated

plasticity using simple pulses of two similar odors failed to reveal any measureable stimulus specificity and it was unclear how the animal could possibly perform the discrimination. However this approach did not present any opportunity for the animal to compare the two odor choices. When we examined responses to odor transitions, to test whether flies compare odors over time, MBON responses were clearly different. These findings show that template mismatch signal conveyed by MBON activity is modulated by the stimulus history of the choices presented to the fly in such a way that it drives the most adaptive behavior. Moreover, behavioral experiments showed that flies only responded distinctly to the two similar odors when they were presented close together in time, providing independent evidence that a temporal comparison is important for discrimination. These results show that a single associative memory can drive different behavioral outcomes, as a result of a choice-dependent modulation of a template mismatch signal.

Results:

Learning in a single MB compartment can support both hard discrimination and generalization.

Previous work has shown that flies are capable of high levels of performance on both hard discrimination and generalization in two-alternative forced choice tasks(Campbell et al. 2013). This study identified a trio of odors to use for experiments on the specificity of memory, based on the degree of overlap of KC response patterns: pentyl acetate (PA) butyl acetate (BA) and ethyl lactate (EL) (Fig. 1A, left). PA and BA are chemically similar and elicit highly overlapping response patterns in the KC population (Campbell et al. 2013). EL is distinct, both chemically and in terms of KC response patterns. Choices between different combinations of these cues can be used to measure memory specificity. Take, for example, an experiment where flies are trained to form an association with PA. We can present flies with a difficult discrimination task by giving them a choice between the similar odors (PA and BA), or an easy discrimination with a choice between the paired odor (PA) and the dissimilar odor (EL). We can also test whether the association with PA generalizes to the similar odor BA, by giving flies a choice between BA and EL. Since we use these odors in many different combinations for different task structures, with and without reciprocal design, here we will use A to refer to the paired odor (PA or BA) and A' to refer to the other similar odor, which is unpaired, while B always refers to the dissimilar odor, EL. With this nomenclature, hard discrimination involves an A versus A' choice, easy discrimination is A versus B and generalization is A' versus B (Fig. 1A).

Although previous work showed flies learn both generalization and discrimination tasks using these odors, electric shock was used as the reinforcement(Campbell et al. 2013). Consequently the synaptic changes responsible were likely distributed across many areas of the mushroom body, and possibly elsewhere. To confine plasticity to a more restricted region of the brain, we used optogenetic reinforcement, pairing the activation of specific DANs with odor presentation (Fig. 1B)(Schroll et al. 2006; Claridge-Chang et al. 2009). We used drivers to express CSChrimson in DANs targeting different compartments involved in aversion learning: α3 (MB630B) and γ2α'1 (MB296B)(Aso, Hattori, et al. 2014; Aso and Rubin 2016). Since compartments have different time courses for memory acquisition and recall(Aso and Rubin

2016), the number of repetitions of odor-reinforcement pairing and the time between training and testing differed depending on the compartment tested (see Methods).

From this set of aversive learning compartments, we identified two with contrasting properties in easy and hard discrimination tasks (Fig. 1C). Flies that received reinforcement from PPL1-α3 were poor at the hard discrimination although they performed well on the easy task (Fig. 1D, $p = 0.007$, $n = 12$). On the other hand, flies that received optogenetic reinforcement via the PPL1-γ2α'1 DAN performed the hard discrimination as effectively as the easy discrimination (Fig. 1E, d, $p = 0.08$, $n = 12$). Conditioning in γ2α'1 enabled equally high performance on the hard and easy discrimination tasks whereas in α3, performance was poorer for hard discrimination.

The difference in the ability to support fine discrimination in these two compartments makes a clear prediction with respect to generalization. In a simple model of template matching, the closer the match to template, the easier the genearlization but the harder the discrimination. Consequently, the weakly discriminating α3 compartment is predicted to support strong performance on generalization, while the strongly discriminating γ2α'1 compartment should not.

We tested this by examining relative performance on generalization and easy discrimination tasks in these two compartments. To keep a parallel structure between experiments, we quantified performance by comparing against control experiments where flies were exposed to the optogenetic stimulation in an unpaired manner, prior to odor delivery (Fig. 1F; see Methods; note that since these experiments did not have reciprocal controls the performance scores in Fig. 1 G-H are computed differently than in Fig. 1 D-E). As expected, training flies using DAN PPL1-α3 yielded similarly high performance on both generalization and easy discrimination tasks (Fig. 1G, $p = 0.31$, $n = 12$). Contrary to our prediction however, we found that flies receiving reinforcement from the DAN PPL1-γ2α'1 generalized effectively, with a performance level indistinguishable from that in the easy discrimination task (Fig. 1H $p = 0.89$, $n = 12$).

Although the experiments above target optogenetic punishment to specific sites within the MB, there is the possibility that there are secondary sites of plasticity that contribute to the behavioral performance we observe, via indirect connections between MB compartments. To more rigorously confine plasticity to γ2α'1, we performed an experiment where dopamine production is restricted solely to the γ2α'1 DAN within the fly. Dopamine is necessary for flies to show any measurable aversive learning(Kim, Lee, and Han 2007; Qin et al. 2012; Aso et al. 2019), and its production requires the *Drosophila* tyrosine hydroxylase enzyme, DTH(Neckameyer and White 1993; Riemensperger et al. 2011; Cichewicz et al. 2016). So we examined performance of flies lacking dopamine biosynthesis throughout the nervous system(Cichewicz et al. 2016), but with production rescued specifically in PPL1-γ2α'1 by driving expression of UAS-DTH using the split hemidrivers TH-DBD and 73F07-AD(Aso et al. 2019). Performance was significantly higher for the DTH-rescue flies than for the mutants (Fig. 1I, $p = 0.038$, $n = 8$), indicating that plasticity in this set of synapses is sufficient for hard discrimination.

These results show that a single memory trace formed via plasticity confined to γ2α'1 supports strong performance on the hard discrimination, and generalization tasks. We note that the choice outcomes of these paradigms are opposite: in the generalization experiments flies distribute away from odor A', while in the hard discrimination task, flies accumulate in the A' quadrant. We next sought to understand how plasticity in a single set of synapses can result in these two distinct modes of recall.

KC inputs to both MB compartments contain enough information for discrimination

We started by evaluating whether the odor inputs to the γ2α'1 and α3 compartments carry enough information to discriminate between the two similar odors used in our behavior experiments. Previous measurements of KC responses to these odors did not distinguish between different KC subtypes (Campbell et al. 2013). We used two-photon calcium imaging (Fig. 2A) to measure cell population responses (Fig. 2B) in the KC subtypes that send axons to γ2α'1 (γ and α'/β' KCs) and α3 (α/β KCs). In separate sets of flies, GCaMP6f (T.-W. Chen et al. 2013) was expressed in γ KCs (d5HT1b (Yuan, Joiner, and Sehgal 2006)), α'/β' KCs (c305a (Armstrong et al. 2006; Krashes et al. 2007)) and α/β KCs (c739 (McGuire, Le, and Davis 2001)). γ and α'/β' KCs had to be imaged separately since there is no driver that exclusively labels both subtypes. As expected, examining the trial-averaged response traces of individual KCs for each of the three subtypes showed that many of the same cells respond to the two similar odors (PA and BA), but representations did not completely overlap (example fly for each subtype in Fig. 2C). Responses were very different for the dissimilar odor, EL. KC population response vectors from single trials, plotted as projections along the first two principal component axes (Fig. 2D), also show the similarity in KC representations between the chemically similar odors. Finally we examined the similarity of responses for individual KCs to the different pairs of odors. Pooling cells across all imaged flies ($n = 7$ flies for γ, 5 for α'/β' and 6 for α/β KCs), we found that similar odors elicited similar response strengths in individual KCs (Supplementary Fig. 1A, γ KCs: $r = 0.74$, $p < 0.001$; α'/β' KCs: $r = 0.76$, $p < 0.001$ and α/β KCs: $r = 0.63$, $p < 0.001$). Correlation coefficients were lower and were not significant for the dissimilar odors (Supplementary Fig. 1B, γ KCs: $r = 0.04$, $p = 0.60$; α'/β' KCs: $r = 0.06$, $p = 0.55$ and α/β KCs: $r = -0.04$, $p = 0.77$).

We next evaluated whether KC odor representations contain enough information to discriminate between the two similar odors. We fitted logistic regression models that take KC population responses as input and determine the probability that a given odor evoked the input activity vector. For example, for a decoder trained to recognize KC activity evoked by PA, we plotted the predicted probability that a given input activity vector was evoked by PA (Supplementary Fig. 2C). Examining decoder accuracy averaged across all trials, for all flies (Fig. 2E), we found that decoder identification accuracies were as high for each similar odor as they were for the dissimilar odor, for γ KCs (comparing accuracies for PA and EL $p = 0.06$, BA-EL $p = 0.08$), α'/β' KCs (PA-EL $p = 0.13$, BA-EL $p = 0.13$) and α/β KCs (PA-EL $p = 0.63$, BA-EL $p = 0.73$). Thus, even in the relatively small sample of cells imaged from each KC subtype, population activity contains enough information to identify the similar odors as accurately as the dissimilar one, for all KC types.

Even though compartments γ2α'1 and α3 receive olfactory input from totally distinct subsets of KCs, we have shown there is enough information for fine discrimination in all three KC subtypes. Is this information retained one synapse downstream, when hundreds of KCs converge onto the MBONs in these two compartments?

Plasticity in MBON γ2α'1 is not sufficiently odor-specific for discrimination

We next wanted to examine plasticity properties downstream of the KCs, in γ2α'1 and whether they enable discrimination between the similar odors. To examine the effect of plasticity on MBON-γ2α'1 activity, we imaged responses pre- and post-pairing odor with optogenetic reinforcement on the microscope (Fig. 3A). γ2α'1 spans parts of both the γ and α' MB lobes, but receives reinforcement from a single DAN, PPL1-γ2α'1(Aso, Hattori, et al. 2014). Two MBONs send dendrites to the same region of neuropil; here we treat them as a single cell type - MBON-γ2α'1. We expressed Chrimson88.tdTomato(Strother et al. 2017) in the DAN PPL1-γ2α'1 (driven by 82C10-LexA which also drives weak expression in compartments α2 and α3(Pfeiffer et al. 2013)) and opGCaMP6f selectively in MBON-γ2α'1 (MB077B, Fig. 3B(Aso, Hattori, et al. 2014)). We imaged MBON-γ2α'1 responses (Fig. 3B, C) to pulses of all three odors, before and after pairing one of the similar odors with optogenetic reinforcement (Fig. 3A). We delivered two repeats of each odor stimulus before and after pairing, and imaged only one, to minimize adaptation effects(Berry, Phan, and Davis 2018). Based on previous studies(Séjourné et al. 2011; Hige, Aso, Modi, et al. 2015; Owald et al. 2015; Cohn, Morantte, and Ruta 2015; Perisse et al. 2016; Berry, Phan, and Davis 2018), we expected to see depression of the MBON-γ2α'1 response specifically (or at least preferentially) for the reinforced odor. However, after pairing, MBON-γ2α'1 responses to A and A' were both strongly depressed (Fig. 3D, E, $p = 0.001$ for A and $p = 0.001$ for A' , $n = 11$ flies). In fact we could not detect a difference in response size between the two similar odors, even though only one (A) had been paired with reinforcement (Fig. 3F, $p = 0.77$). As expected, responses to the dissimilar odor (B) were not affected ($p = 0.18$).

With such strong depression of MBON-γ2α'1 responses to both similar odors, how do flies discriminate between them after learning? We postulated that the apparent discrepancy between our behavioral observations and measurements of MBON activity might be because we did not adequately reproduce the fly's sensory experience when it is choosing between a pair of odors at an odor boundary.

Odor transitions modulate the mismatch readout

When flies make a choice between two odors in the behavioral arena, they encounter an odor boundary. As they traverse this boundary, the concentration of one odor drops away, and that of the other rises (Supplementary Fig. 2A). To mimic this experience while imaging neural activity on the microscope, we designed an odor delivery system capable of generating odor stimuli with rapid transitions from one odor to another. We characterized the performance of this odor delivery system with a photo-ionization detector to measure odor concentration changes and an anemometer to measure airflow (Supplementary Fig. 2B-D).

We next repeated the experiment, examining plasticity in MBON-γ2α'1, but now using odor stimuli that more closely mimic what the fly experiences in the arena. The pairing trials were the same as in the experiments described in Fig. 3, where a single odor pulse was presented during pairing (Fig. 4A, detailed protocol in Supplementary Fig. 3A). These mimicked behavioral conditioning, when the entire arena was flooded with the paired odor (odor A) during optogenetic reinforcement (as in Fig. 1B, middle). But in this case, rather than using single odor pulses to characterize pre- and post-pairing responses, we presented odor transitions to mimic odor boundary crossings in the arena. (Fig. 1B, right). Unlike our results with single pulses, with these test stimuli we saw a dramatic modulation of the MBON response i.e. the mismatch signal. Surprisingly, the depression of responses to A' seen in single pulses was not detectable in an A to A' transition. Responses were similar to pre-pairing levels when A' was preceded by A, but not when the order was reversed (Fig. 4B). We quantified this effect by computing MBON response size to the second pulse for the different transition orders (Fig. 4C). As expected, when odor A came second responses were significantly lower after pairing. In contrast, when A' was second, responses were similar pre- and post-pairing ($p = 0.376$). Above, we found that when each odor was presented singly, post-pairing responses to A and A' were too similar to be distinguished (Fig. 3). However, when we made the analogous comparison when each odor came second in a transition, we observed that post-pairing responses to A' were now significantly larger than to A (Supplementary Fig. 3C, $n=13$, $p = 0.001$). These results show a significant effect of stimulus history on responses to the unpaired odor A'.

To better capture the change in MBON response around the odor transition, we computed a contrast score. After learning, contrast around the odor transition was higher when transitioning into odor A' than into odor A (Supplementary Fig. 3D, $p = 0.001$). To confirm the change in MBON responses to transitioning odors was due to optogenetic reinforcement, we did control experiments where LED stimulation was omitted and found no significant difference pre- and post- no-LED, mock pairing trials (Supplementary Fig. 4; $n = 14$ flies).

We observed a modulation of the γ2α'1 template mismatch signal that depended on an odor transition that mimics a specific odor choice. When A' is presented in isolation, post-pairing responses are depressed and not measurably different from responses to A (Fig. 3D-F). This would allow flies to generalize learning between these odors in most circumstances. But when A' comes in a transition after A, MBON-γ2α'1 responses are larger. This allows the similar odor to be discriminated from the paired odor. One strong prediction of these results is that if this modulation is the basis of discrimination, it should not occur in the α3 compartment, where reinforcement does not enable flies to discriminate between the similar odors.

No mismatch signal modulation in the weakly discriminating α3 compartment

We decided to look for modulation of the mismatch signal in MBON-α3 by imaging responses to odor transitions. α3 is a slow-learning compartment, when an odor is paired with α3 reinforcement via DAN PPL1-α3, behavioral performance gradually rises until it peaks 24 hours later(Aso and Rubin 2016). So we chose to train flies in a behavior chamber, by pairing an odor with a shock reinforcement and imaged MBON-α3 responses to transitioning odor stimuli 20 -

28 hours later (Fig. 4D, detailed protocol in Supplementary Fig. 3B). This experimental approach, based on maximizing behavioral performance, did not permit us to measure pre- and post-learning responses in the same fly. So in these experiments, we compared responses observed after pairing in one cohort of flies with those in a mock-trained cohort, where shock was delivered at a different time than odor (Supplementary Fig. 3B).

We found that in response to odor transitions, there was no mismatch signal modulation in MBON-α3 (Fig. 4E). Responses to the second odor in the transition were depressed for both transition orders (A' to A, $p < 0.001$, pooled n = 14 PA-paired and n = 12 BA-paired flies; A to A', $p < 0.001$) (Fig. 4F). As expected, responses to the dissimilar odor (odor B) showed no significant depression ($p = 0.48$). To evaluate how this affected odor edge detection, we computed the contrast score as we did for MBON-γ2α'1. With MBON-α3,- we saw very little contrast at the transition point, and contrast was similarly low for either order of the transition (Supplementary Fig. 4E, $p = 0.86$).

Transition effects on KC odor responses are not sufficient to support hard discrimination.

We have shown that MBON-γ2α'1 responses show modulation of the mismatch signal at odor transitions, but MBON-α3 does not. Early sensory processing in the antennal lobe could alter odor representations when delivered as transitions(Saha et al. 2013; Nizampatnam et al. 2018). So we examined responses to odor transitions in the input KC populations for MBON-γ2α'1 (γ and α'/β' KCs) and MBON-α3 (α/β KCs) (Fig. 5A). We attempted to use the KC activity patterns we measured to reproduce our observations of MBON activity. Specifically, we used logistic regression models, adjusting the weights of KC inputs so that model outputs were low for A and A' and high for B. We only used single pulse data to train the models to match the training procedure used with flies in the behavior and MBON activity experiments. To ensure we did not penalize cells that responded uniquely to transitions, weights were initialized at 1 and we trained models without any weight regularization. Trained weights were negatively correlated with responses to A, as expected (Fig. 5B, top, Pearson correlation coefficient for γ KCs = - 0.402, α'/β' = - 0.274 and α/β = - 0.211). These weights were then used to calculate model output for A'-A and A-A' transitions. Model outputs were not significantly different between the two directions of the transitions, and were low for both (Fig 5B). We also trained a separate set of models on single pulse as well as odor transition data, to verify that KC activity contained enough information to discriminate A'-A from A-A' (Fig. 5C). We found that the odor transition stimulus responses from all three KC subtypes could be used to discriminate between them. Models fitted to sensory representations can only discriminate transitions if explicitly trained to do so, but flies do not need such explicit training. We concluded that the pairing-dependent modulation of the mismatch signal we observed in MBON-γ2α'1 activity arises downstream of KCs.

Overall, these results show that a single set of changed synapses - one engram - is read out by the γ2α'1 network in two different ways, depending on the choice given to the fly. These observations lead us to the prediction that even if an engram is formed in γ2α'1, flies would only

be able to discriminate odors if they experienced odor transitions. We tested this prediction with behavioral experiments using odor sequences.

Odor sequences show that a temporal comparison contributes to odor discrimination.
We have shown that MBON-γ2α'1 responses to the similar odors only became distinguishable when presented as transitions. We predicted that flies' behavioral response to the paired and unpaired odors should also be indistinguishable, unless they are encountered as transitions. Further, since MBON-γ2α'1 signals positive valence (Aso, Sitaraman, et al. 2014), our activity measurements predict that flies might be attracted to A' if they encounter an A to A' transition. To test these predictions, we examined behavioral responses to temporal sequences of odor, converting a spatial border into an odor transition in time. Flies were trained in the circular arena, and then tested by flooding the entire arena with a sequence of odor pulses. This enabled us to control when flies encountered an odor transition, and also to interrupt transitions with 25s of clean air. We determined the timing of odor pulse transitions using PID measurements at the exhaust outlet of the arena (Supplementary figure 6A), and analyzed fly behavior around these timepoints.

Attraction to an odor was quantified by how much the flies move upwind; in the arena odors flow inwards from the periphery so we measured displacement away from the center of the arena. We examined the time course of upwind displacement for direct and interrupted transitions (Fig. 6 A-D). We observed strong upwind displacement when there was a direct transition from A to A' (Fig. 6 A). This is consistent with our observation that MBON-γ2α'1, a positive valence MBON that drives upwind behavior (unpublished communication - Yoshinori Aso), is highly active during these transitions. In fact, the mean upwind displacement after an A-A' transition was similar to that caused by optogenetic activation of MBON-γ2α'1 in the arena (Fig. 6 F). However, when transitions were interrupted by a 25s air period, upwind displacements in response to the second pulse were not significantly different (Fig. 6 C, D, F, n unpaired = 12, n paired = 13, $p = 0.85$). Additionally no significant upwind behavior was observed when the sequence was reversed, in an A' to A transition, again consistent with the plasticity we observed in our imaging experiments (Fig. 6 B).

One possible explanation for these results is that flies start further downwind when they experience the A-A' transition, and so have more space to go upwind in the arena. However, starting locations at the onset of the second odor pulse were not significantly different for either transition order, for both direct and interrupted transitions (Supplementary Figure 6B n unpaired = 12, n paired = 12, $p = 0.08$ for direct; n = 12, 13, $p = 0.39$ for interrupted).

We also wanted to rule out the possibility that the increased upwind displacement during a transition comes from a linear combination of the response to the end of the first odor pulse and the beginning of the second. We summed the pulse1 off response (Supplementary Figure 6C) and pulse2 on response (Supplementary Figure 6D) in interrupted transition experiments to get the linear-summed displacement curves for the paired and unpaired, similar odors (Supplementary Figure 6E). The experimentally measured displacement time course for A' to A

transitions was very close to the linear sum (Supplementary figure 6E-F, bottom). However, for A to A' transitions, although both curves were initially similar, at later time points the observed displacement was higher than the linear sum (Supplementary figure 6E-F, top). Quantifying the upwind displacements averaged over the entire odor period confirmed these observations. There was a significantly greater displacement for the direct A to A' transitions than expected from linear summation (Supplementary figure 6G, $n = 12$, $p = 0.001$). This was not the case for the reverse A' to A transitions ($n = 12$, $p = 0.09$), where the linear sum actually tended to be higher. We concluded that flies exhibit an attraction response to the unpaired odor (A') but only when stimulus history is such that follows the paired odor (A).

These results show that a single memory trace in the γ2α'1 compartment can be recalled in two different ways, depending on immediate stimulus history. When the two odors are encountered well-separated in time, both MBON-γ2α'1 output and fly behavior are indistinguishable for the two similar odors. However, when they are closely apposed in time, MBON-γ2α'1 activity is enhanced and flies are attracted to the unpaired, similar odor.

Discussion:

Using a pair of perceptually similar odors (A and A') and one distinct odor (B), we identified a site in the mushroom body circuit that supports similar levels of behavioral performance in both discrimination and generalization tasks. We showed that learning-related synaptic plasticity results in neuronal responses to the similar odors that are both depressed and very similar to each other when presented in isolation, consistent with the strong generalization. However, when the cues were presented in transitions, as at an odor boundary, neuronal responses were distinct. Behavioral experiments using carefully timed odor delivery showed that flies' response to A' was distinct from A only if they were delivered in a transition. These results demonstrate how the choice of cues presented to the animal can influence the behavioral outcome of these types of tasks. An odor boundary presents an opportunity to compare those choices, and a form of learning-dependent modulation of the template mismatch signal amplifies the small differences between them to serve as the basis for discrimination.

Different Mechanisms of Flexible Memory Recall

Flexibility of memory recall can be achieved in many ways, depending on the circuit and the context. One common solution is to add a layer of contextual modulation to gate memory recall. In Drosophila, recalling food reward associations from one MB compartment is gated by another MB compartment depending on whether or not the fly is hungry(Perisse et al. 2016). In this case, recall is regulated by neuropeptide signaling that couples neural activity to satiety state. Ongoing motor activity can also affect dopaminergic inputs along the MB lobes (Cohn, Morantte, and Ruta 2015). These could modulate memory recall on relatively short timescales based on the behavioral state of the animal. However, to implement choice-dependent recall, the stimuli themselves need to be the source of the modulating signal.

Another solution for implementing flexible memory recall could be to form multiple parallel memory traces with different properties. For example, when flies learn an odor-sugar association, the sweet taste drives synaptic changes in one compartment, which holds a short-term memory of the association, while the caloric content of the reward induces plasticity in a separate compartment that supports longer-term memory (Huetteroth et al. 2015; Yamagata et al. 2015). These parallel memories can be recalled independently(Trannoy et al. 2011). However, there are no known mechanisms that would allow the options available to the animal to influence which memory trace dominates a recall event. Interestingly, other experiments have shown that long-term memory is also less specific than recent or short term memory (Ichinose et al. 2015; König et al. 2017). This dichotomy also seems relevant here - the MBON supporting the less specific memory, MBON-α3, is also a long-term memory compartment. Perhaps selection pressures operating on long-term memories tend to favor generalization since the array of choices available may shift considerably over the course of the memory. Conversely the selection pressure for fine discrimination may be stronger in short-term environment situations, where it may be more likely that extremely similar options are present at the same time. Nevertheless, the situation we study here calls for an even higher level of flexibility than either of these two broad mechanisms - contextual modulation and parallel memory traces - could likely achieve. No matter how many options can be available to an animal, the most adaptive choice is always the cue with the highest subjective value.

The selectivity of memory has traditionally been thought of as residing in the odor representations carried by the KCs. However below we argue that the specificity is not only a function of which synapses are modified by also the network's dynamic state at the time of recall.

Template matching and MBON activity as a 'mismatch signal'

The stimulus specificity of memory is generally conceptualized as a template matching process. According to this model, an internally memorized template of the associated cue is created during memory formation. Incoming sensory input is then compared against this template and, for a cue whose match-to-template is above some threshold, that cue elicits the learned response.

Studies of olfactory learning in Drosophila have yielded a clear understanding of the nature of the template in the mushroom body. Pairing odor with reinforcement depresses the synapses of a sparse set of responding KCs, creating a learned template of the reinforced odor(Berry, Phan, and Davis 2018; Cohn, Morantte, and Ruta 2015; Hige, Aso, Modi, et al. 2015; Owald et al. 2015; Perisse et al. 2016; Séjourné et al. 2011). Downstream MBON activity reflects the overlap between different odor response patterns in the KCs - strongly overlapping odors elicit reduced MBON responses, as observed here and in previous work (Hige, Aso, Modi, et al. 2015) others. In other words, post-training MBON activity reflects the extent of template mismatch. Indeed, it was possible to use the extent of overlap between different odor response patterns in the KCs to predict whether an association formed with one odor will generalize to an overlapping test odor (Campbell et al. 2013). Conversely, discrimination must be based on non-overlap i.e. KCs that

respond uniquely to one of the stimuli being distinguished. This predicts there would be an inherent trade-off between performance on these two types of tasks: the more overlapping two stimuli are, the easier the generalization but the harder the discrimination (Barak, Rigotti, and Fusi 2013). However, we found that flies can perform both tasks with similar levels of efficiency, consistent with results in other systems (C. Chen, Krueger-Burg, and de Hoz 2019). This was the case even though we targeted plasticity to a single site in the MB using optogenetic training. Furthermore, when we restricted dopamine biosynthesis strictly to that site within the fly brain, performance was still high on both tasks. This argues against the possibility that the discrimination-generalization trade-off is resolved by forming multiple memory traces with different stimulus specificity, one supporting discrimination, one for generalization. Instead, our data supports the notion that the animal can use a single memory trace flexibly, switching behavioral responses depending on the option available i.e. choosing to avoid A over A', but A' over B.

One engram, multiple modes of recall based on stimulus comparisons

If an animal's choice behavior is influenced by the options available, it follows that there must be some kind of comparison between those choices. Using odor sequences revealed that this comparison is facilitated when the two stimuli come close together in time. When we presented the two similar odors as solitary pulses, functional imaging experiments in MBON-γ2α'1 showed extremely similar, strongly depressed response patterns. Presumably responses to the two odors were not identical, but the overlap between KC response patterns was so high that we could not measure the difference in MBON activity after training. However when the two stimuli were presented in sequence, the responses were very distinct. When the odor sequence transitioned from A to A', the response to A' was much stronger than when that odor was presented in isolation. Evaluating the change in neural activity around the odor transition point was particularly revealing. Neural activity in MBON-γ2α'1 was strongly modulated during the transition, the response time course clearly capturing a difference between the similar odors for the A to A' transition. However for MBON-α3, from the compartment that did not strongly support fine discrimination, the contrast around the odor transition was extremely poor, and unlikely to be adequate for discriminating between the similar odors. These results show that stimulus history accentuates contrast, and that this correlates with whether or not a compartment supports fine discrimination.

Our results from functional imaging were strongly corroborated by independent behavioral experiments. When flies were trained by targeting reinforcement to the strongly discriminating compartment with PPL1-γ2α'1, we could detect no difference in the behavioral responses to the two similar odors when they were presented in isolation. However when juxtaposed in time as odor sequences, a clear difference was observed. When flies experienced a direct transition from odor A to A', they responded to A' with upwind movement, a behavioral signature of attraction to odor. This is consistent with the strong MBON-γ2α'1 activity we observed in our corresponding imaging experiments - this MBON signals positive valence and optogenetic activation of this cell drives a similar upwind behavior (Aso, Sitaraman, et al. 2014). These results indicate that, when trained to avoid odor A and presented with a choice between A and

A', the choice to avoid A is actually accentuated by an increase in the attraction to A'. This is reminiscent of results from studies in fly larvae (Y.-C. Chen and Gerber 2014; Mishra, Louis, and Gerber 2010) and adults (Barth et al. 2014) which found that flies discriminate more finely if trained to form an aversive association using a differential conditioning paradigm, where one stimulus is paired with punishment, followed by presentation of a second stimulus without any reinforcement. Differential training yielded stronger discrimination than a protocol that omits the second stimulus. This was, in part, because flies learned that the unpaired odor represents safety. This is quite similar to our results, which also used differential conditioning. The transition-dependent approach behavior we observed could be interpreted as learning that the unpaired odor is 'safe'.

Enhanced template mismatch signal arises downstream of sensory representations

KC activity forms a useful template for memory because different activity patterns are so well separated (Honegger, Campbell, and Turner 2011), which arises in part because of the highly stochastic connectivity of inputs to the MB (Caron et al. 2013). This pattern separation allows synaptic changes to be highly stimulus specific (Olshausen and Field 1996). However, some information about odor similarity is retained - activity patterns are not so sparse that pattern separation is complete (Campbell et al. 2013; Hige, Aso, Rubin, et al. 2015; Dasgupta, Stevens, and Navlakha 2017; Endo, Tsuchimoto, and Kazama 2020). Prior work did not examine whether the low level of correlation that exists is distributed differentially across different KC subtypes. These subtypes, γ, α/β and α'/β' KCs differ primarily in their axonal projections but also exhibit differences in their dendritic inputs (Li et al. 2020; Strausfeld, Sinakevitch, and Vilinsky 2003; Zheng et al. 2018), suggesting the possibility that pattern separation is strong in some subtypes but weak in others. Since the two MBONs we studied, MBON-γ2α'1 and MBON-α3 receive input from completely distinct sets of KCs, we examined odor representations in each of the three major KC subtypes. There are well-established differences between these subtypes in terms of their rates of spontaneous firing (Turner, Bazhenov, and Laurent 2008), spike thresholds and connectivity with inhibitory inputs (Inada, Tsuchimoto, and Kazama 2017). Additionally, KC subtypes can have different integrative properties; the α/β core subset of KCs integrates inputs on a timescale different from other KC subtypes, in a manner that is highly predictive of behavioral choice(Groschner et al. 2018). Despite these differences, we show that in each of the three major subtypes of KCs, odor representations retain information about similarity, and are also able to support discrimination between the pair of similar odors we used.

Although a template of comparable specificity seems to be established in each KC subtype, we also examined whether stimulus history exerts different effects on the template comparison in different KC subtypes. Prior work has shown history-dependent effects at multiple layers of the olfactory circuit. For example, in the rodent olfactory bulb, responses to odor sequences are linear combinations of the responses to individual pulses(Gupta, Albeanu, and Bhalla 2015). On the other hand, in locusts, presenting odors singly or in transitions altered odor representations in KCs and upstream(Broome, Jayaraman, and Laurent 2006), and the extent of response alteration correlated with the accuracy of behavioral recall to a conditioned odor(Saha et al. 2013). In Drosophila, odor transitions can cause similar changes in PN representations that

result in altered innate odor preference(Badel et al. 2016). In another locust study, (Nizampatnam et al. 2018), presenting an odor in a transition altered its representation to enhance contrast in the locust antennal lobe glomeruli. We examined whether KC population responses to transitions could account for the MBON responses we observed. We found that that although odor representations are altered when they are delivered as transitions, this is not sufficient to enable hard discrimination. Mimicking the training given to flies, we trained logistic regression models to respond to single pulse stimuli and found that unlike flies, they could not discriminate between the two transition stimuli. Thus sensory representations for odors in transitions do not diverge sufficiently to allow hard discrimination. We conclude that the effect on MBON-γ2α'1 activity we observe must occur either at or downstream of KC-MBON synapses.

How does the mushroom body network modulate the MBON response to A' depending on recent stimulus history? We have established a few important constraints on a possible mechanism: i) it occurs at or downstream of KC>MBON synapses ii) it arises after learning and iii) it only occurs asymmetrically, in A to A' transitions and not the reverse. The extent of depression of KC>MBON synapses is inevitably slightly weaker for any test odor that overlaps imperfectly with the learned template. Therefore, the circuit must compare the small differences in MBON activity before and after odor transitions, and amplify only small, upward steps in activity.

Many possible mechanisms could potentially implement this. For example, training could change MBON-γ2α'1 activity at the offset selectively for the paired odor, increasing the response to any stimulus that follows. Another class of mechanisms could make an explicit comparison of MBON activities in time, before and after the transition, using a delay-line (Schöneich, Kostarakos, and Hedwig 2015; Sullivan and Konishi 1986). A real-time and a delayed copy of MBON-γ2α'1 activity could be appropriately summed and amplified to generate a sequence-specific positive feed-back signal for the γ2α'1 MBONs. In an alternative, purely feed-forward scheme, a separate compartment would also have to undergo plasticity during training, and serve as the source of inputs to the delay-line system. Although our TH-rescue experiment does not support this model, we cannot formally rule out that another compartment undergoes plasticity driven by a co-transmitter in DANs (Aso et al. 2019).

Some of these proposed mechanisms rely on additional circuitry beyond just the input KCs, MBON-γ2α'1 and DAN PPL1-γ2α'1. Connectomics studies have identified the other circuit elements with projections in the γ2α'1 compartments. There is a DAN, PAM-γ4<γ1γ2 that receives input in γ2, and connects to MBON-γ4>γ1γ2, which in turn feeds back onto the γ2 compartment (Aso, Hattori, et al. 2014; Li et al. 2020). As MBON-γ4>γ1γ2 is glutamatergic, its direct action on MBON-γ2α'1 is expected to be inhibitory (Li et al. 2020). MBON-γ2α'1 also receives input from the MB-intrinsic anterior paired lateral (APL) and dorsal paired medial (DPM) neurons. Both these neurons have intermingled input/output sites that are thought to process signals locally, likely within a compartment (Li et al. 2020). Finally, another MB output neuron, MBON-γ1γ2, receives some input that overlaps with MBON-γ2α'1, however it forms no direct connections with γ2α'1 MBONs (Li et al. 2020). Future studies can use this anatomical information to begin to explore candidate mechanisms for the modulation of mismatch we report

in this study. Additionally, we note that although the potential mechanisms described above are easier to conceptualize at the circuit level, they could also be implemented in a neuron-intrinsic manner via intracellular signaling mechanisms.

A model for memory based on a static template, established during training, recalled the same way on every encounter of the paired stimulus is an over-simplification. An association assigns valence or meaning to a stimulus. But valence is subjective and ever-changing, based on an animal's internal state, or on ongoing events in its environment. Our study has revealed a novel way to modulate how well a test stimulus matches a learned template based on ongoing stimulus dynamics. This is an important step to move beyond a plasticity-centric view of memory recall.

Methods

Fly strains

Drosophila melanogaster were raised on standard cornmeal food at 21 ℃ at 60% relative humidity on standard cornmeal food on a 12-12h light-dark cycle. For optogenetics behavior experiments, crosses were set on food supplemented with 0.2mM all-trans-retinal and moved to 0.4mM after eclosion and kept in the dark throughout.

Transgene	**Expression target/reporter description**	**Bloomington stock number, reference**
MB296B split Gal4	DAN PPL1-γ2α'1	BDSC:68253(Aso and Rubin 2016)
MB630B split Gal4	DAN PPL1-α3	BDSC:68290(Aso and Rubin 2016)
d5HT1b-Gal4	γ KCs	BDSC:27637(Yuan, Joiner, and Sehgal 2006)
c305a-Gal4	α'/β' KCs	BDSC:30829(Krashes et al. 2007)
c739-Gal4	α/β KCs	BDSC:7362(McGuire, Le, and Davis 2001)
MB077B split Gal4	MBONs γ2α'1	BDSC:68283(Aso, Hattori, et al. 2014)
MB082C split Gal4	MBONs α3	BDSC:68286(Aso, Hattori, et al. 2014)
R82C10-LexA	DANs PPL1-γ2α'1, α2, α3	BDSC:54981(Pfeiffer et al. 2013)
20XUAS-CsChrimson-mVenus attp18	Optogenetic activation for behavior	BDSC:55134(Klapoetke et al. 2014)
13XLexAop2-IVS-Syn21-Chrimson88-tdT-3.1-P10	Optogenetic activation for imaging	BDSC: n.a.(Strother et al. 2017)
20XUAS-IVS-Syn21-opGCaMP6f-P10	Codon-optimized Ca^{2+} reporter	BDSC: n.a.(T.-W. Chen et al. 2013)

Expression patterns of split-GAL4 lines produced by Janelia FlyLight(Jenett et al. 2012) can be viewed online (http://splitgal4.janelia.org/cgi-bin/splitgal4.cgi).

Behavior
DAN driver split Gal4 crossed with 20XUAS-CsChrimson-mVenus attp18

TH-rescue experiment (genetic strategy as in(Aso et al. 2019)**)**
knockout
w, 20XUAS-CSChrimson-mVenus attP18; +; ple^2, DTHFS± BAC attP2, TH-ZpGAL4DBD VK00027/ TM6B

crossed with

w; R73F07-p65ADZp attP40/ CyO; ple^2, DTHFS± BAC attP2/ TM6B

knockout and rescue in DAN PPL1-γ2α'1
w, 20XUAS-CSChrimson-mVenus attP18; UAS-DTH1m; ple^2, DTHFS± BAC attP2, TH-ZpGAL4DBD VK00027/ TM6B

crossed with

w; R73F07-p65ADZp attP40/ CyO; ple^2, DTHFS± BAC attP2/ TM6B

KC imaging:
γ KCs: w; +/+; d5HT1b-Gal4/ 20XUAS-IVS-Syn21-opGCaMP6f-P10 VK00005
α'/β' KCs: w; c305a-Gal4/+; 20XUAS-IVS-Syn21-opGCaMP6f-P10 VK00005/+
α/β KCs: w; c739-Gal4/+; 20XUAS-IVS-Syn21-opGCaMP6f-P10 VK00005/+

MBON γ2α'1 imaging:
20XUAS-IVS-Syn21-opGCaMP6f-P10 Su(Hw)attP8/ w; R25D01-ZpGAL4DBD attP40/ 82C10-LexAp65 attP40; R19F09-p65ADZp attP2/ 13XLexAop2-IVS-Syn21-Chrimson88::tdT-3.1-p10 in VK00005

R25D01 and R19F09 are components of the MB077B stable split-GAL4 driver (BDSC: 68283)

MBON α3 imaging:
w; +/+; 20XUAS-IVS-Syn21-opGCaMP6f-P10 VK00005/ R23C06-ZpGAL4DBD in attP2, R40B08-p65ADZp VK00027

R23C06 and R40B08 are components of the MB082C stable split-GAL4 driver (BDSC: 68286)

Behavior Experiments

Odor quadrant choice assay: Groups of approximately 20 females, aged 4-10 d post-eclosion were anaesthetized on a cold plate and collected at least two day prior to experiments. After a day of recovery on 0.4 mM all-trans-retinal food, they were transferred to starvation vials containing nutrient-free agarose. Starved females were trained and tested at 25 ℃ at 50% relative humidity in a dark circular arena described in(Aso and Rubin 2016). The arena consisted of a circular chamber surrounded by four odor delivery ports that divide the chamber into quadrants. The input flow rate through each port was 100 mL/min, which was actively vented out a central exhaust at 400 mL/min. Odors were pentyl acetate, butyl acetate and ethyl lactate (Sigma-Aldrich product numbers 109584, 287725, and W244015 respectively). Except for the TH-rescue experiments shown in Fig. 1I, these odors were diluted 1:10000 in paraffin oil (Sigma-Aldrich product number 18512). For the experiments in Fig. 1I, we used a different odor delivery system which utilizes air dilution of saturated odorant vapor, and delivered odors at a 1:16 dilution of saturated vapor.

Flies were aspirated into the arena via a small port, and allowed 60 s to acclimatize before training commenced. Training consisted of exposing the flies to one of the odors while providing optogenetic stimulation via a square array of red LEDs (617 nm peak emission, Red-Orange LUXEON Rebel LED, 122 lm at 700mA) which shone through an acrylic diffuser to illuminate flies from below. LED activation consisted of 30 pulses of 1s duration with a 1s inter-flash interval, commencing 5s after switching on the odor valves and terminating 5s after valve shut-off.

To optimize learning scores, we used different training regimes depending on the compartments receiving optogenetic reinforcement, according to(Aso and Rubin 2016). A single training session was used for MB296B, TH-mutant, TH-rescue, while 3 training sessions, separated by 60 seconds, were used for some MB296B experiments, as indicated in the text. For MB630B we used 10 training sessions separated by 15 minutes.

Following training, testing was carried out with the appropriate odors for each task. In the test configuration, the two different odor choices are presented in opposing quadrants for 60 s. Videos of fly behavior were captured at 30 frames per second using MATLAB (Mathworks, USA) and BIAS (http://archive.iorodeo.com/content/basic-image-acquisition-software-bias.html) and analyzed using custom-written code in MATLAB.

Odor attraction assay: For the odor attraction assay, the outputs of odor machines were re-configured to inject the output of a single odor machine into all four quadrants. We switched output from one machine to the other to deliver rapid odor transitions in time. About 15 flies were introduced into the arena for each experiment. The rest of the behavioral procedures were identical to those used in the quadrant choice assay.

Optogenetic MBON-activation assay: For this assay, a clean air stream was delivered into all four arena quadrants throughout the experiment. Flies expressed CSChrimson in MBON γ2α'1. Flies received six 10 s long LED flashes, separated by 60s of darkness. The rest of the behavioral procedures were identical to those used in the quadrant choice assay.

Calcium imaging

Flies were imaged on a resonant-scanning, Janelia, jET MIMMS2.0 custom-designed two-photon microscope, with a Chameleon Ultra II, Titanium-sapphire laser (Coherent, USA) tuned to emit 920 nm. Images were acquired using a 20x, NA 1.0, water-immersion objective lens XLUMPLFLN (Olympus, Japan) and a GaAsP PMT H11706P-40 SEL (Hamamatsu, Japan). Power after the objective ranged from 4-5 mW for MBON imaging and 4-7 mW for KC imaging, depending on the preparation. Microscope control and data acquisition ran on the Scanimage platform (Vidrio, USA). Frames were acquired at 30 Hz, but three frames at a time were averaged during acquisition, for a final frame rate of 10 Hz. For KC imaging, pixels were sampled at 0.22 µm/pixel and for MBON imaging, at 0.18 µm/pixel. For photostimulation, flies were fully illuminated from beneath with 617 nm light through a liquid light-guide (LLG-03-59-340-0800-2, Mightex, USA) butt-coupled to an LED light source (GCS-0617-04-A0510, Mightex, USA). Intensity at the fly was 1 mW/mm^2. LED pulses were delivered at a frequency of 1 Hz, with a duty-cycle of 50%, for 5s, starting 2s after paired-odor onset.

For optogenetics imaging experiments, crosses were set on food supplemented with 0.4mM all-trans-retinal, and maintained on the same food at 25° C until flies were used for experiments. Flies were prepared as described previously(Honegger, Campbell, and Turner 2011; Campbell et al. 2013). 3 to 8 day old female flies were immobilized in a 0.25 mm thick stainless-steel sheet with a photo-chemically etched tear-drop shaped hole (PhotoFab, UK) and glued into place with two-component epoxy (Devcon, USA). For imaging in the KC somata and the MBON dendrites, head angle was adjusted differently to give best optical access to the target region, taking care to keep the antennae dry beneath the metal plate. For KC and MBON α3 imaging, the back of the head was submerged in Ringer's bath solution consisting in mM: NaCl, 103; KCl, 3; CaCl2, 1.5; MgCl2, 4; NaHCO3, 26; N-tris(hydroxymethyl) methyl-2-aminoethane-sulfonic acid, 5; NaH2PO4, 1; trehalose, 10; glucose, 10 (pH 7.3, 275 mOsm). For γ2α'1 MBON experiments, the flies were starved (24 hours in nutrient-free, distilled-water agarose vials). Previous studies have shown that hemolymph sugar is halved in flies starved for 24 hrs(Dus et al. 2011). So we used bath Ringer's where glucose and trehalose were halved to 5 mM each and the non-metabolizable sugar arabinose (10 mM) was substituted to maintain osmolarity. For KC imaging, once the brain was exposed, bath solution was momentarily aspirated away and the preparation was covered in a drop of 5% (w/v) agarose (Cambrex Nusieve, catalog #50080) in Ringer's, cooled to 36° C, which was then flattened with a 5 mm diameter circular coverslip that was then removed just prior to imaging.

For KC imaging, 8 repeats of single odor pulses and each kind of odor transition were delivered with an inter trial interval of 45 s. Stimulus types were randomly interleaved. For MBON γ2α'1 imaging, we delivered two repeats of either single odor pulses or transitions before and after odor-reinforcement pairing (Supplementary Fig. 4, A-B, adapted from Berry *et al.*, 2018(Berry,

Phan, and Davis 2018). Only one repeat was imaged before and after pairing. For MBON α3 imaging, only the second presentation of each transition stimulus type was imaged.

Odor delivery for imaging experiments

To deliver rapid odor transitions, we set up two separate odor delivery machines(Honegger, Campbell, and Turner 2011) and joined their outputs upstream of the final tube delivering odor to the fly. These systems use saturated odor vapor which is then serially diluted in clean air to a final dilution of 0.8% (v/v). This was delivered to the fly at a flow rate of 400 mL/min from a tube with an inner diameter of 3 mm.

We measured relative odor concentrations with a photoionization detector (200B miniPID, Aurora Scientific, Canada). Different chemical vapors at the same concentration generate different PID signal amplitudes. Thus, the PID signal is linearly related to concentration only for a given odor chemical. The PID probe was used to measure and tune odor pulse shapes and to measure and account for the time taken for an odor pulse to reach the fly. The short period of overlap between the fall of the first odor pulse and the rise of the second occurred for both kinds of transition stimuli, paired to unpaired transitions and unpaired to paired transitions (Fig. 4, supplement 1 C). Hence, this overlap would not affect our measures of discriminability between the two similar odors. A hot-wire anemometer S490 (Kurz, USA) was used to measure air-velocity at a sampling rate of 10 KHz while mock-odor pulses were being delivered though empty odor-vials. This was to rule out any mechanical transients at the time of odor-transitions being an external cue to the flies. To minimize transients, we combined the steps of the second serial dilution of the second odor pulse and mixing the outputs of the two odor machines. The second pulse in all transition stimuli was introduced into the final air stream at one-tenth the flow-rate. Any pressure-transients due to valve switches during the transition to the second pulse were too small to be measured by the anemometer in the final output.
We saw a small valve-switching transient at the beginning of the first pulse in any transition (8% the size of the steady-state flow, Fig. 4 supplement 1, D). Since this transient was always at the onset of the first pulse, and not during transitions, again, it did not affect discriminability.

Data Analysis

Behavior:

Videos recorded during the test phase were analyzed using custom-written MATLAB code. The centroid of each fly was identified and the number of centroids in each quadrant computed for every frame of the experiment.

For discrimination experiments, a Performance Index (PI) was calculated as the number of flies in the quadrants containing the paired odor minus the number in the quadrants with the unpaired odor, divided by the total number of flies(Tully and Quinn 1985). This value was calculated for every frame of the movie, and the values over the final 30 s of the test period averaged to compute a single PI. Discrimination experiments employed a reciprocal design where the identity of the paired and unpaired odors was swapped and a single data point represents the averaged PI from two reciprocally trained groups of flies.

Generalization experiments could not employ a reciprocal design, so instead we compared scores against control experiments where flies were exposed to LED stimulation that was not paired with odor delivery; instead stimulation preceded odor by 2 min. In this case the PI score reported as a single data point is the PI observed from the generalization experiment minus the PI observed in the unpaired control.

Statistical testing was done as described in figure legends. We used the non-parametric, independent sample, Wilcoxon rank sum test to compare performance indices across treatment groups. Statistical testing was performed with custom code written in Matlab (Mathworks, USA). The appropriate sample size was estimated based on the standard deviation of performance indices in previous studies using the same assay(Aso and Rubin 2016).

For the odor attraction and the MBON-activation assays, computing upwind displacement required us to track each fly's trajectory in time. We used the Caltech Fly Tracker(Eyjolfsdottir et al. 2014) to automatically extract fly trajectories from videos. Odor stimulus onset time in the arena was determined from PID measurements of odor concentration at the arena exhaust port. For the MBON-activation assay, stimulus onset was set as the moment the LED turned on. Upwind displacement was computed as the increase in the distance from the center for each fly, relative to its location at stimulus onset, for each time-point over the entire stimulus window. The displacement for all flies in an arena experiment were then averaged before plotting and statistical testing.

Calcium imaging: For KC data, fluorescence time-series images were first analyzed with the Suite2P analysis pipeline(Pachitariu et al. 2016) running in Matlab to register data and identify active single-cell regions of interest (ROIs). For MBON imaging data, ROIs were manually drawn using a custom Matlab script. For both types of experiments, average, raw fluorescence intensity for each ROI was then extracted by a separate, custom script. A background region with no labeling in each imaging field was manually defined, and background fluorescence (this consisted of the PMT offset and autofluorescence) was subtracted from all measured fluorescence values for that field. ΔF/F was computed according to the following equation

$$\Delta F/F_i = (F_i - F_0)/F_0$$

where Fi is the fluorescence of a given cell ROI at a given time-point in a trial, and F_0 is the same ROI's fluorescence in an 8 s window during the baseline period on that trial, prior to odor delivery. For all plotted fluorescence traces, ΔF/F time-series data was boxcar filtered with a window-width of 0.2 s. All other analysis was done with un-filtered ΔF/F data. For making statistical comparisons, ΔF/F values during stimulus presentation were averaged over time windows as indicated in each figure.

KC population activity decoders: The objective of this analysis was to determine whether a linear classifier can discriminate trials of a particular odor based on the KC responses. We fitted logistic regression models to predict whether or not KC activity on a given trial was evoked by a

particular odor. For example, an odorA classifier received KC population activity vectors as input and then made a prediction whether the input activity was evoked by odorA/not odorA. Separate classifiers were fitted for each fly, for each odor. We used leave-one-out cross validation (LOOCV): of the 8 repeats acquired for each odor, one was left out as a test trial and the remaining trials were used to fit the model. In this way, we systematically fitted models for each combination of training and test trail sets. All plotted accuracy scores are for model predictions on test trials not used for fitting.
The cost function used to estimate goodness of fit was the binary cross-entropy with a quadratic regularization, defined as

$$cost = -\frac{1}{m}\sum_{i=1}^{m} y_i \times log(h_i) - (1 - y_i) \times log(1 - h_i) + \frac{\lambda}{2m}\sum_{j=1}^{n} \theta_j^2$$

where m is the number of training trials, y_i is the correct odor label for a given trial (0 or 1), h_i is the model's prediction (or probability that the input activity vector was in response to a given odor) for the same trial, λ is the regularization constant (we used $\lambda = 1$, but this was not a sensitive parameter), n is the number of neurons in a given dataset and θ_j are the weights of the neurons. For logistic regression models fitted without regularization (shown in Fig. 5 B), λ was set to 0.

The model's prediction, h was computed according to the equation

$$h = \frac{1}{1 + e^{-(X \times \theta)}}$$

Where X is the $m \times n$ activity matrix for m training trials and θ is the $n \times 1$ vector of weights.

Acknowledgements:
This work was supported by the Howard Hughes Medical Institute and the National Institutes of Health (2R01DC010403-06). We thank Florin Albeanu and the Albeanu group for hosting MM for part of the time that this work was carried out, and also for engaging in helpful discussions and feedback. Robert Eifert at Cold Spring Harbor Laboratory and Steven Sawtelle, Igor Negrashov, Vasily Goncharov and others at jET, Janelia Research Campus provided vital technical support. Todd Laverty and others in the Janelia Drosophila resources team provided support with fly lines and media. Gudrun Ihrke and others in Project Technical Resources provided support with expression characterization. We also thank all members of the Turner and Aso groups and Eyal Gruntman, Vivek Jayaraman, Ann Hermundstad, Florin Albeanu and Priyanka Gupta for support, discussions and feedback.

Author contributions

MNM, AR, HR, YA and GCT all contributed to writing the manuscript and conceptualizing data

analysis. MNM, AR, YA and GCT conceptualized the study and planned experiments. AR and YA did behavior experiments and MNM did imaging experiments.

Competing interests statement

The authors have no competing interests to declare.

Data availability statement

The datasets generated during and/or analyzed during the current study are available from the corresponding author on reasonable request.

Code availability statement

The custom Matlab code used for analysis in this manuscript will be made available upon request during the process of peer review. If accepted, commented code with instructions on how to run it will be made publicly available as a code repository.

References

Armstrong, J. D., M. J. Texada, R. Munjaal, D. A. Baker, and K. M. Beckingham. 2006. "Gravitaxis in Drosophila Melanogaster: A Forward Genetic Screen." *Genes, Brain, and Behavior* 5 (3): 222–39.

Aso, Yoshinori, Kornelia Grübel, Sebastian Busch, Anja B. Friedrich, Igor Siwanowicz, and Hiromu Tanimoto. 2009. "The Mushroom Body of Adult Drosophila Characterized by GAL4 Drivers." *Journal of Neurogenetics* 23 (1-2): 156–72.

Aso, Yoshinori, Daisuke Hattori, Yang Yu, Rebecca M. Johnston, Nirmala A. Iyer, Teri-T B. Ngo, Heather Dionne, et al. 2014. "The Neuronal Architecture of the Mushroom Body Provides a Logic for Associative Learning." *eLife* 3 (December): e04577.

Aso, Yoshinori, Robert P. Ray, Xi Long, Daniel Bushey, Karol Cichewicz, Teri-Tb Ngo, Brandi Sharp, et al. 2019. "Nitric Oxide Acts as a Cotransmitter in a Subset of Dopaminergic Neurons to Diversify Memory Dynamics." *eLife* 8 (November). https://doi.org/10.7554/eLife.49257.

Aso, Yoshinori, and Gerald M. Rubin. 2016. "Dopaminergic Neurons Write and Update Memories with Cell-Type-Specific Rules." *eLife* 5 (JULY): 1–15.

Aso, Yoshinori, Divya Sitaraman, Toshiharu Ichinose, Karla R. Kaun, Katrin Vogt, Ghislain Belliart-Guérin, Pierre-Yves Plaçais, et al. 2014. "Mushroom Body Output Neurons Encode Valence and Guide Memory-Based Action Selection in Drosophila." *eLife* 3 (December). https://doi.org/10.7554/eLife.04580.

Badel, Laurent, Kazumi Ohta, Yoshiko Tsuchimoto, and Hokto Kazama. 2016. "Decoding of Context-Dependent Olfactory Behavior in Drosophila." *Neuron* 91 (1): 155–67.

Barak, Omri, Mattia Rigotti, and Stefano Fusi. 2013. "The Sparseness of Mixed Selectivity Neurons Controls the Generalization-Discrimination Trade-Off." *The Journal of Neuroscience: The Official Journal of the Society for Neuroscience* 33 (9): 3844–56.

Barnstedt, Oliver, David Owald, Johannes Felsenberg, Clifford B. Talbot, Paola N. Perrat, and Scott Waddell. 2016. "Memory-Relevant Mushroom Body Output Synapses Are Cholinergic Article Memory-Relevant Mushroom Body Output Synapses Are Cholinergic." *Neuron*, 1–11.

Barth, Jonas, Shubham Dipt, Ulrike Pech, Moritz Hermann, Thomas Riemensperger, and André Fiala. 2014. "Differential Associative Training Enhances Olfactory Acuity in Drosophila Melanogaster." *The Journal of Neuroscience: The Official Journal of the Society for Neuroscience* 34 (5): 1819–37.

Berry, Jacob A., Anna Phan, and Ronald L. Davis. 2018. "Dopamine Neurons Mediate Learning and Forgetting through Bidirectional Modulation of a Memory Trace." *Cell Reports* 25 (3): 651–62.e5.

Broome, Bede M., Vivek Jayaraman, and Gilles Laurent. 2006. "Encoding and Decoding of Overlapping Odor Sequences." *Neuron* 51 (4): 467–82.

Campbell, R. A. A., K. S. Honegger, H. Qin, W. Li, E. Demir, and G. C. Turner. 2013. "Imaging a Population Code for Odor Identity in the Drosophila Mushroom Body." *Journal of Neuroscience* 33 (25): 10568–81.

Caron, Sophie J. C., Vanessa Ruta, L. F. Abbott, and Richard Axel. 2013. "Random Convergence of Olfactory Inputs in the Drosophila Mushroom Body." *Nature* 497 (7447): 113–17.

Chen, Chi, Dilja Krueger-Burg, and Livia de Hoz. 2019. "Wide Sensory Filters Underlie Performance in Memory-Based Discrimination and Generalization." *PloS One* 14 (4): e0214817.

Chen, Tsai-Wen, Trevor J. Wardill, Yi Sun, Stefan R. Pulver, Sabine L. Renninger, Amy Baohan, Eric R. Schreiter, et al. 2013. "Ultrasensitive Fluorescent Proteins for Imaging Neuronal

Activity.” *Nature* 499 (7458): 295–300.
Chen, Yi-Chun, and Bertram Gerber. 2014. “Generalization and Discrimination Tasks Yield Concordant Measures of Perceived Distance between Odours and Their Binary Mixtures in Larval Drosophila.” *The Journal of Experimental Biology* 217 (Pt 12): 2071–77.
Cichewicz, K., E. J. Garren, C. Adiele, Y. Aso, Z. Wang, M. Wu, S. Birman, G. M. Rubin, and J. Hirsh. 2016. “A New Brain Dopamine-Deficient Drosophila and Its Pharmacological and Genetic Rescue.” *Genes, Brain, and Behavior* 16 (3): 394–403.
Claridge-Chang, Adam, Robert D. Roorda, Eleftheria Vrontou, Lucas Sjulson, Haiyan Li, Jay Hirsh, and Gero Miesenböck. 2009. “Writing Memories with Light-Addressable Reinforcement Circuitry.” *Cell* 139 (2): 405–15.
Cohn, Raphael, Ianessa Morantte, and Vanessa Ruta. 2015. “Coordinated and Compartmentalized Neuromodulation Shapes Sensory Processing in Drosophila.” *Cell* 163 (7): 1742–55.
Crittenden, J. R., E. M. Skoulakis, K. A. Han, D. Kalderon, and R. L. Davis. 1998. “Tripartite Mushroom Body Architecture Revealed by Antigenic Markers.” *Learning & Memory* 5 (1-2): 38–51.
Dasgupta, Sanjoy, Charles F. Stevens, and Saket Navlakha. 2017. “A Neural Algorithm for a Fundamental Computing Problem.” *Science* 358 (6364): 793–96.
Dus, Monica, Soohong Min, Alex C. Keene, Ga Young Lee, and Greg S. B. Suh. 2011. “Taste-Independent Detection of the Caloric Content of Sugar in Drosophila.” *Proceedings of the National Academy of Sciences of the United States of America* 108 (28): 11644–49.
Endo, Keita, Yoshiko Tsuchimoto, and Hokto Kazama. 2020. “Synthesis of Conserved Odor Object Representations in a Random, Divergent-Convergent Network.” *Neuron* 108 (2): 367–81.e5.
Eyjolfsdottir, Eyrun, Steve Branson, Xavier P. Burgos-Artizzu, Eric D. Hoopfer, Jonathan Schor, David J. Anderson, and Pietro Perona. 2014. “Detecting Social Actions of Fruit Flies.” In *Computer Vision – ECCV 2014*, 772–87. Springer International Publishing.
Groschner, Lukas N., Laura Hak Wah Chan, Rafal Bogacz, Dasgupta Shamik, and Gero Miesenböck. 2018. “Dendritic Integration of Sensory Evidence in Article Dendritic Integration of Sensory Evidence in Perceptual Decision-Making.” *Cell*, 1–12.
Gupta, Priyanka, Dinu F. Albeanu, and Upinder S. Bhalla. 2015. “Olfactory Bulb Coding of Odors, Mixtures and Sniffs Is a Linear Sum of Odor Time Profiles.” *Nature Neuroscience* 18 (2): 272–81.
Hare, Todd A., Wolfram Schultz, Colin F. Camerer, John P. O’Doherty, and Antonio Rangel. 2011. “Transformation of Stimulus Value Signals into Motor Commands during Simple Choice.” *Proceedings of the National Academy of Sciences of the United States of America* 108 (44): 18120–25.
Hige, Toshihide, Yoshinori Aso, Mehrab N. Modi, Gerald M. Rubin, and Glenn C. Turner. 2015. “Heterosynaptic Plasticity Underlies Aversive Olfactory Learning in Drosophila.” *Neuron* 88 (5): 985–98.
Hige, Toshihide, Yoshinori Aso, Gerald M. Rubin, and Glenn C. Turner. 2015. “Plasticity-Driven Individualization of Olfactory Coding in Mushroom Body Output Neurons.” *Nature* 526 (7572): 258–62.
Honegger, K. S., R. A. A. Campbell, and G. C. Turner. 2011. “Cellular-Resolution Population Imaging Reveals Robust Sparse Coding in the Drosophila Mushroom Body.” *Journal of Neuroscience* 31 (33): 11772–85.
Hopfield, J. J. 1982. “Neural Networks and Physical Systems with Emergent Collective Computational Abilities.” *Proceedings of the National Academy of Sciences of the United States of America* 79 (8): 2554–58.
Huetteroth, Wolf, Emmanuel Perisse, Suewei Lin, Martín Klappenbach, Christopher Burke, and Scott Waddell. 2015. “Sweet Taste and Nutrient Value Subdivide Rewarding Dopaminergic

Neurons in Drosophila." *Current Biology: CB* 25 (6): 751–58.
Hunt, Laurence T., Nils Kolling, Alireza Soltani, Mark W. Woolrich, Matthew F. S. Rushworth, and Timothy E. J. Behrens. 2012. "Mechanisms Underlying Cortical Activity during Value-Guided Choice." *Nature Neuroscience* 15 (3): 470–76, S1–3.
Ichinose, Toshiharu, Yoshinori Aso, Nobuhiro Yamagata, Ayako Abe, Gerald M. Rubin, and Hiromu Tanimoto. 2015. "Reward Signal in a Recurrent Circuit Drives Appetitive Long-Term Memory Formation." *eLife* 4 (November). https://doi.org/10.7554/eLife.10719.
Inada, Kengo, Yoshiko Tsuchimoto, and Hokto Kazama. 2017. "Origins of Cell-Type-Specific Olfactory Processing in the Drosophila Mushroom Body Circuit." *Neuron* 95 (2): 357–67.e4.
Ito, K., K. Suzuki, P. Estes, M. Ramaswami, D. Yamamoto, and N. J. Strausfeld. 1998. "The Organization of Extrinsic Neurons and Their Implications in the Functional Roles of the Mushroom Bodies in Drosophila Melanogaster Meigen." *Learning & Memory* 5 (1-2): 52–77.
Jenett, Arnim, Gerald M. Rubin, Teri-T B. Ngo, David Shepherd, Christine Murphy, Heather Dionne, Barret D. Pfeiffer, et al. 2012. "A GAL4-Driver Line Resource for Drosophila Neurobiology." *Cell Reports* 2 (4): 991–1001.
Kim, Young-Cho, Hyun-Gwan Lee, and Kyung-An Han. 2007. "D 1 Dopamine Receptor dDA1 Is Required in the Mushroom Body Neurons for Aversive and Appetitive Learning in Drosophila." *Journal of Neuroscience* 27 (29): 7640–47.
Klapoetke, Nathan C., Yasunobu Murata, Sung Soo Kim, Stefan R. Pulver, Amanda Birdsey-Benson, Yong Ku Cho, Tania K. Morimoto, et al. 2014. "Independent Optical Excitation of Distinct Neural Populations." *Nature Methods* 11 (3): 338–46.
König, Christian, Emmanuel Antwi-Adjei, Mathangi Ganesan, Kasyoka Kilonzo, Vignesh Viswanathan, Archana Durairaja, Anne Voigt, and Ayse Yarali. 2017. "Aversive Olfactory Associative Memory Loses Odor Specificity over Time." *The Journal of Experimental Biology* 220 (Pt 9): 1548–53.
Krashes, Michael J., Alex C. Keene, Benjamin Leung, J. Douglas Armstrong, and Scott Waddell. 2007. "Sequential Use of Mushroom Body Neuron Subsets during Drosophila Odor Memory Processing." *Neuron* 53: 103–15.
Li, Feng, Jack W. Lindsey, Elizabeth C. Marin, Nils Otto, Marisa Dreher, Georgia Dempsey, Ildiko Stark, et al. 2020. "The Connectome of the Adult Drosophila Mushroom Body Provides Insights into Function." *eLife* 9 (December). https://doi.org/10.7554/eLife.62576.
Lin, Andrew C., Alexei M. Bygrave, Alix de Calignon, Tzumin Lee, and Gero Miesenböck. 2014. "Sparse, Decorrelated Odor Coding in the Mushroom Body Enhances Learned Odor Discrimination." *Nature Neuroscience* 17 (4): 559–68.
Lin, Hui-Hao, Jason Sih-Yu Lai, An-Lun Chin, Yung-Chang Chen, and Ann-Shyn Chiang. 2007. "A Map of Olfactory Representation in the Drosophila Mushroom Body." *Cell* 128 (6): 1205–17.
McGuire, S. E., P. T. Le, and R. L. Davis. 2001. "The Role of Drosophila Mushroom Body Signaling in Olfactory Memory." *Science* 293 (5533): 1330–33.
Mishra, Dushyant, Matthieu Louis, and Bertram Gerber. 2010. "Adaptive Adjustment of the Generalization-Discrimination Balance in Larval Drosophila." *Journal of Neurogenetics* 24 (3): 168–75.
Miura, Keiji, Zachary F. Mainen, and Naoshige Uchida. 2012. "Odor Representations in Olfactory Cortex: Distributed Rate Coding and Decorrelated Population Activity." *Neuron* 74 (6): 1087–98.
Modi, Mehrab N., Yichun Shuai, and Glenn C. Turner. 2020. "The Drosophila Mushroom Body: From Architecture to Algorithm in a Learning Circuit." *Annual Review of Neuroscience* 43 (July): 465–84.
Neckameyer, W. S., and K. White. 1993. "Drosophila Tyrosine Hydroxylase Is Encoded by the Pale Locus." *Journal of Neurogenetics* 8 (4): 189–99.

Nizampatnam, Srinath, Debajit Saha, Rishabh Chandak, and Baranidharan Raman. 2018. “Dynamic Contrast Enhancement and Flexible Odor Codes.” *Nature Communications* 9 (1): 3062.
Olshausen, B. A., and D. J. Field. 1996. “Emergence of Simple-Cell Receptive Field Properties by Learning a Sparse Code for Natural Images.” *Nature* 381 (6583): 607–9.
Owald, David, Johannes Felsenberg, Clifford B. Talbot, Gaurav Das, Emmanuel Perisse, Wolf Huetteroth, and Scott Waddell. 2015. “Activity of Defined Mushroom Body Output Neurons Underlies Learned Olfactory Behavior in Drosophila.” *Neuron* 86 (2): 417–27.
Pachitariu, Marius, Carsen Stringer, Sylvia Schröder, Mario Dipoppa, L. Federico Rossi, Matteo Carandini, and Kenneth D. Harris. 2016. “Suite2p: Beyond 10,000 Neurons with Standard Two-Photon Microscopy.” *bioRxiv*.
Perisse, Emmanuel, David Owald, Oliver Barnstedt, Clifford B. Talbot, Wolf Huetteroth, and Scott Waddell. 2016. “Aversive Learning and Appetitive Motivation Toggle Feed-Forward Inhibition in the Drosophila Mushroom Body.” *Neuron* 90 (5): 1086–99.
Pfeiffer, B. D., T. B. Ngo, K. L. Hibbard, C. Murphy, A. Jenett, and J. W. Truman. 2013. “LexA Driver Collection of Rubin Laboratory at Janelia Farm.” *Personal Communication to FlyBase*.
Plaçais, Pierre-Yves, Séverine Trannoy, Anja B. Friedrich, Hiromu Tanimoto, and Thomas Preat. 2013. “Two Pairs of Mushroom Body Efferent Neurons Are Required for Appetitive Long-Term Memory Retrieval in Drosophila.” *Cell Reports* 5 (3): 769–80.
Qin, Hongtao, Michael Cressy, Wanhe Li, Jonathan S. Coravos, Stephanie A. Izzi, and Joshua Dubnau. 2012. “Gamma Neurons Mediate Dopaminergic Input during Aversive Olfactory Memory Formation in Drosophila.” *Current Biology: CB* 22 (7): 608–14.
Riemensperger, Thomas, Guillaume Isabel, Hélène Coulom, Kirsa Neuser, Laurent Seugnet, Kazuhiko Kume, Magali Iché-Torres, et al. 2011. “Behavioral Consequences of Dopamine Deficiency in the Drosophila Central Nervous System.” *Proceedings of the National Academy of Sciences of the United States of America* 108 (2): 834–39.
Saha, Debajit, Kevin Leong, Chao Li, Steven Peterson, Gregory Siegel, and Baranidharan Raman. 2013. “A Spatiotemporal Coding Mechanism for Background-Invariant Odor Recognition.” *Nature Neuroscience* 16 (12): 1830–39.
Schöneich, Stefan, Konstantinos Kostarakos, and Berthold Hedwig. 2015. “An Auditory Feature Detection Circuit for Sound Pattern Recognition.” *Science Advances* 1 (8): e1500325.
Schroll, Christian, Thomas Riemensperger, Daniel Bucher, Julia Ehmer, Thomas Völler, Karen Erbguth, Bertram Gerber, et al. 2006. “Light-Induced Activation of Distinct Modulatory Neurons Triggers Appetitive or Aversive Learning in Drosophila Larvae.” *Current Biology: CB* 16 (17): 1741–47.
Seger, Carol A. 2008. “How Do the Basal Ganglia Contribute to Categorization? Their Roles in Generalization, Response Selection, and Learning via Feedback.” *Neuroscience and Biobehavioral Reviews* 32 (2): 265–78.
Séjourné, Julien, Pierre-Yves Plaçais, Yoshinori Aso, Igor Siwanowicz, Séverine Trannoy, Vladimiros Thoma, Stevanus R. Tedjakumala, et al. 2011. “Mushroom Body Efferent Neurons Responsible for Aversive Olfactory Memory Retrieval in Drosophila.” *Nature Neuroscience* 14 (7): 903–10.
Shepard, R. N. 1987. “Toward a Universal Law of Generalization for Psychological Science.” *Science* 237 (4820): 1317–23.
Stahl, Aaron, Nathaniel C. Noyes, Tamara Boto, Valentina Botero, Connor N. Broyles, Miao Jing, Jianzhi Zeng, et al. 2022. “Associative Learning Drives Longitudinally Graded Presynaptic Plasticity of Neurotransmitter Release along Axonal Compartments.” *eLife* 11 (March). https://doi.org/10.7554/eLife.76712.
Strausfeld, Nicholas J., Irina Sinakevitch, and Ilya Vilinsky. 2003. “The Mushroom Bodies of Drosophila Melanogaster: An Immunocytological and Golgi Study of Kenyon Cell

Organization in the Calyces and Lobes." *Microscopy Research and Technique* 62 (2): 151–69.
Strother, James A., Shiuan-Tze Wu, Allan M. Wong, Aljoscha Nern, Edward M. Rogers, Jasmine Q. Le, Gerald M. Rubin, and Michael B. Reiser. 2017. "The Emergence of Directional Selectivity in the Visual Motion Pathway of Drosophila." *Neuron* 94 (1): 168–82.e10.
Sullivan, W. E., and M. Konishi. 1986. "Neural Map of Interaural Phase Difference in the Owl's Brainstem." *Proceedings of the National Academy of Sciences of the United States of America* 83 (21): 8400–8404.
Takemura, Shin-Ya, Yoshinori Aso, Toshihide Hige, Allan Wong, Zhiyuan Lu, C. Shan Xu, Patricia K. Rivlin, et al. 2017. "A Connectome of a Learning and Memory Center in the Adult Drosophila Brain." *eLife* 6 (July). https://doi.org/10.7554/eLife.26975.
Tanaka, Nobuaki K., Hiromu Tanimoto, and Kei Ito. 2008. "Neuronal Assemblies of the Drosophila Mushroom Body." *The Journal of Comparative Neurology* 508 (5): 711–55.
Tenenbaum, J. B., and T. L. Griffiths. 2001. "Generalization, Similarity, and Bayesian Inference." *The Behavioral and Brain Sciences* 24 (4): 629–40; discussion 652–791.
Trannoy, Séverine, Christelle Redt-Clouet, Jean-Maurice Dura, and Thomas Preat. 2011. "Parallel Processing of Appetitive Short- and Long-Term Memories In Drosophila." *Current Biology: CB* 21 (19): 1647–53.
Tully, T., and W. G. Quinn. 1985. "Classical Conditioning and Retention in Normal and Mutant Drosophila Melanogaster." *Journal of Comparative Physiology. A, Sensory, Neural, and Behavioral Physiology* 157 (2): 263–77.
Turner, Glenn C., Maxim Bazhenov, and Gilles Laurent. 2008. "Olfactory Representations by Drosophila Mushroom Body Neurons." *Journal of Neurophysiology* 99 (2): 734–46.
Xu, Wei, and Thomas C. Südhof. 2013. "A Neural Circuit for Memory Specificity and Generalization." *Science* 339 (6125): 1290–95.
Yamagata, Nobuhiro, Toshiharu Ichinose, Yoshinori Aso, Pierre-Yves Plaçais, Anja B. Friedrich, Richard J. Sima, Thomas Preat, Gerald M. Rubin, and Hiromu Tanimoto. 2015. "Distinct Dopamine Neurons Mediate Reward Signals for Short- and Long-Term Memories." *Proceedings of the National Academy of Sciences* 112 (2): 578–83.
Yuan, Quan, William J. Joiner, and Amita Sehgal. 2006. "A Sleep-Promoting Role for the Drosophila Serotonin Receptor 1A." *Current Biology: CB* 16 (11): 1051–62.
Zheng, Zhihao, J. Scott Lauritzen, Eric Perlman, Camenzind G. Robinson, Matthew Nichols, Daniel Milkie, Omar Torrens, et al. 2018. "A Complete Electron Microscopy Volume of the Brain of Adult Drosophila Melanogaster." *Cell* 174 (3): 730–43.e22.

Figure 1:

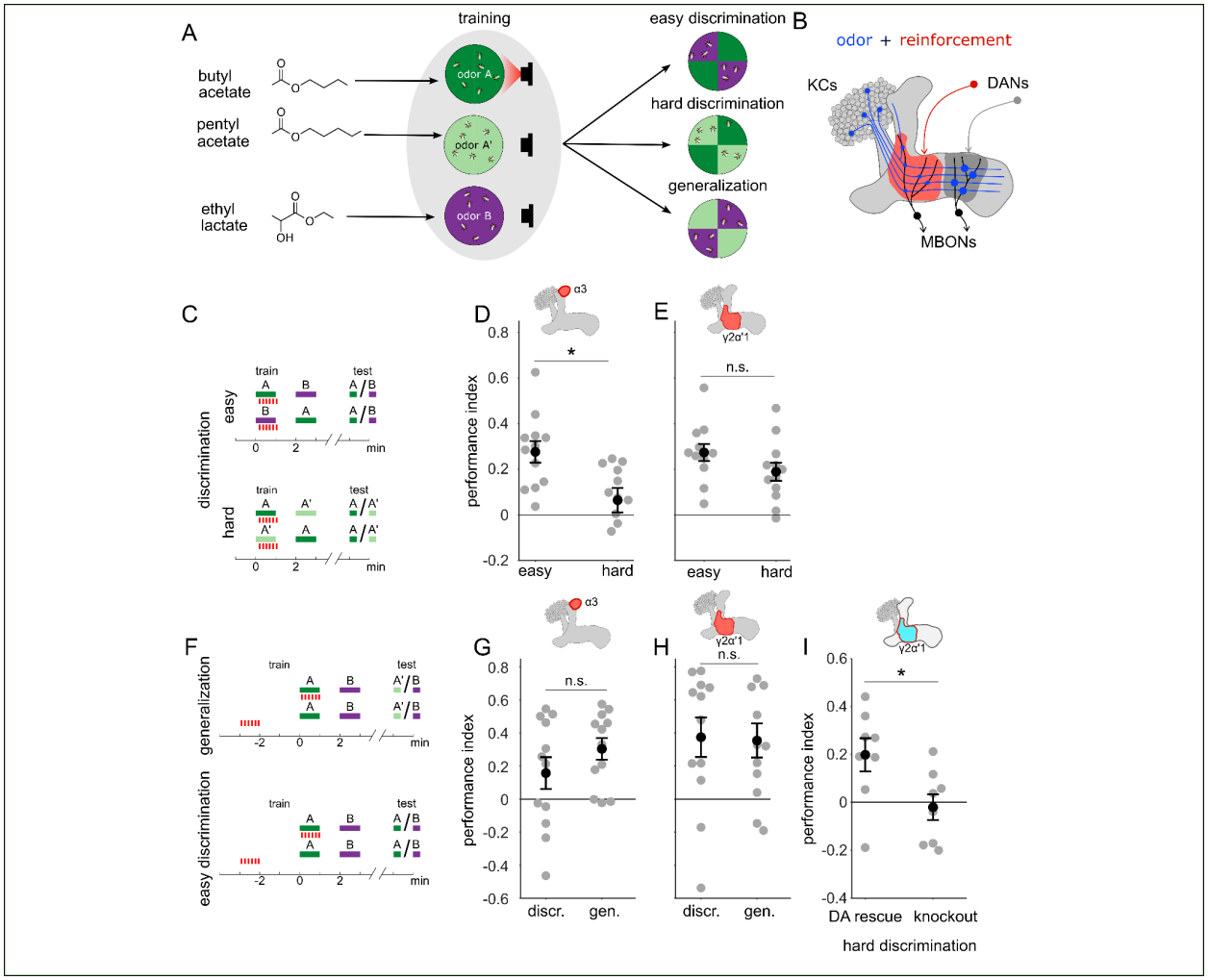

A single set of changed synapses can result in generalization or discrimination

A Left: Chemical structures of the three odors used in the study, the similar odors butyl acetate (BA) and pentyl acetate (PA) and the dissimilar odor ethyl lactate (EL). Middle: During training the similar odors are interchangeably used as the odors that are paired (A) or unpaired (A') with optogenetic reinforcement (LED). Right: Trained flies are then given one of three different choices between odors in opposing arena quadrants. These choices represent the three kinds of tasks used here to study memory specificity. Performance index measures the bias in the distribution of flies across the different quadrants (see Methods).

B Mushroom body learning schematic. KCs activated by an odor (blue) form synapses on MBONs in two compartments (red and gray shading). Reinforcement stimulates the DAN projecting to one compartment (red) leading to synaptic depression.

C Behavior protocols for discrimination tasks at two levels of difficulty. Colored bars represent odor delivery periods, red dashes indicate LED stimulation for optogenetic reinforcement. A represents the paired odor, A' the similar odor and B the dissimilar odor.

D Significantly lower performance on the hard discrimination task with reinforcement to α3 ($p = 0.007$, $n = 12$). Flies received 10 cycles of training and were tested for memory 24 hours later. CsChrimson-mVenus driven in DAN PPL1-α3 by MB630B-Gal4.
E No significant difference in performance on easy versus hard discrimination with reinforcement to γ2α'1 ($p=0.08$, $n = 12$ reciprocal experiments). Flies received 3 cycles of training and were tested for memory immediately after. CsChrimson-mVenus driven in DAN PPL1 γ2α'1 by MB296B-Gal4.
F Behavior protocol for generalization. Scores here are compared to a control protocol where light stimulation is not paired with odor presentation in time.
G No significant difference in performance on generalization and easy discrimination with reinforcement to α3 ($p = 0.31$, $n = 12$). Flies received 10 cycles of training and were tested 24 hours later.
H No significant difference in performance on generalization and easy discrimination with reinforcement to γ2α'1 ($p = 0.89$, $n = 12$ unpaired control performance scores). Flies received 3 cycles of training and were tested immediately after.
I Rescue of the dopamine biosynthesis pathway in DAN PPL1-γ2α'1 is sufficient for performance on the hard discrimination task ($p = 0.04$, $n = 8$).
Black circles and error bars are mean and SEM. Statistical comparisons made with an independent sample Wilcoxon rank sum test.

Figure 2:

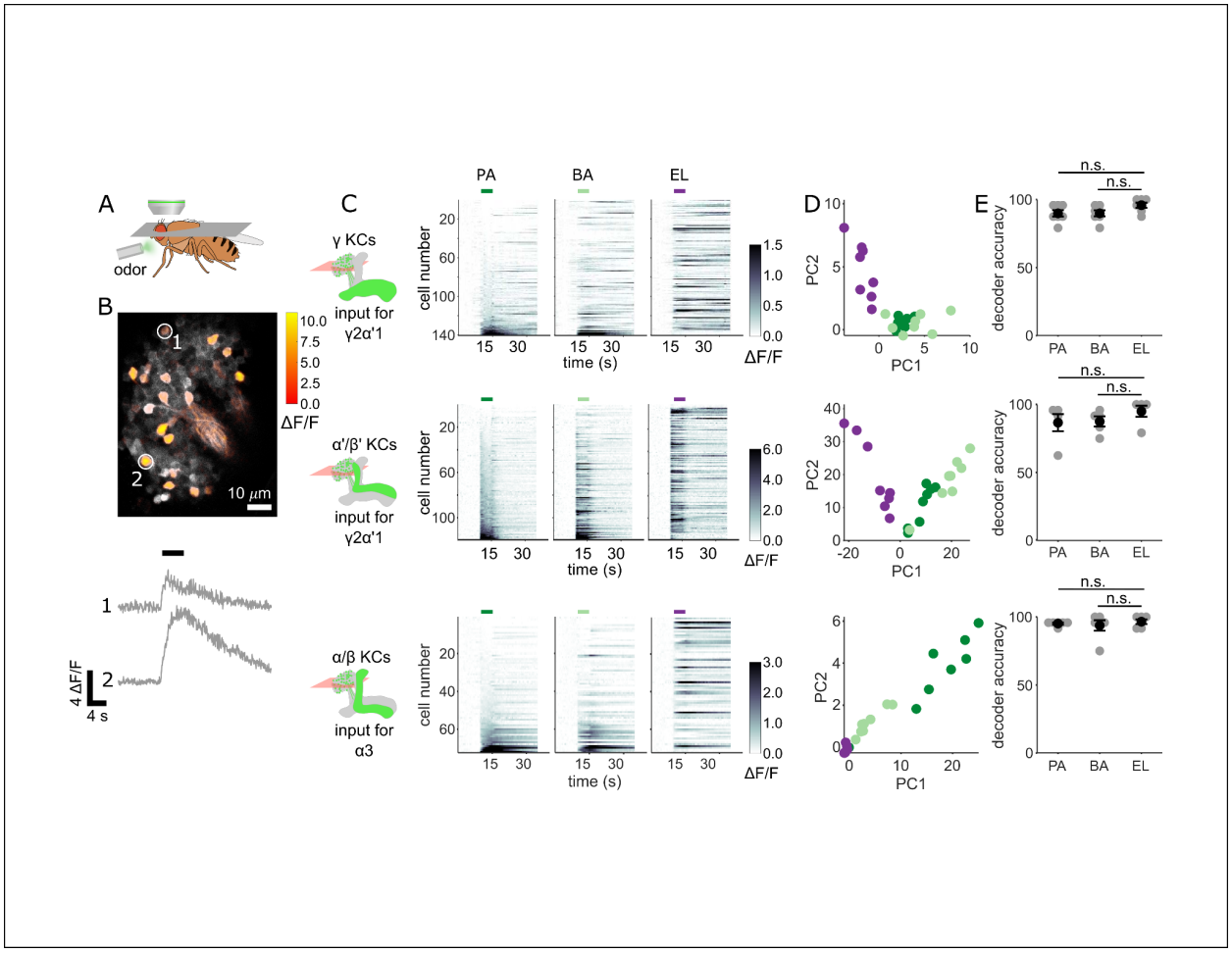

KC responses to single odor pulses contain enough information to discriminate similar odors

A Schematic of in vivo imaging preparation.

B Example single trial odor response patterns in α/β KCs. ΔF/F responses (color bar) are shown overlaid on baseline fluorescence (grayscale). Numbered circles indicate cells for which ΔF/F traces are plotted below. Black bar indicates odor delivery.

C ΔF/F responses of different KC subtypes to the three odors used in this study. Rows show responses of individual KCs, averaged across trials, sorted by responses to PA. GCaMP6f was driven in γ KCs by d5HT1b-Gal4, in α'/β' KCs by c305a-Gal4 and in α/β KCs by c739-Gal4. Colored bars above plots indicate the odor delivery period.

D Odor response patterns for the same example flies as in **C**, projected onto the first two principal component axes to show relative distances between representations for the different odors.

E Decoder prediction accuracies, plotted across flies. Each gray circle is the accuracy of the decoder for one fly for a given odor, averaged across all trials. Black circles and error bars are means and SEM. For γ KCs (top), decoder accuracies for PA (n = 7 flies, p = 0.06) and BA (p = 0.08) were not significantly different from EL accuracy. This was also true for α'/β' KCs (middle, n = 5 flies, p = 0.13 for the PA-EL comparison and p = 0.13 for BA-EL) and α/β KCs (bottom, n = 6 flies, p = 0.63 for PA-EL and p = 0.73 for BA-EL). All statistical testing was done with a paired-sample, Wilcoxon signed rank test with a Bonferroni-Holm correction for multiple comparisons.

C, **D** In this figure, each shade of green denotes one of the two similar odor chemicals. But in subsequent figures, the darker shade represents the odor paired with reinforcement and the lighter shade, the unpaired, similar odor. In the reciprocal design we use, each of the odor chemicals is the paired odor in half the experimental repeats.

Supplementary figure 1:

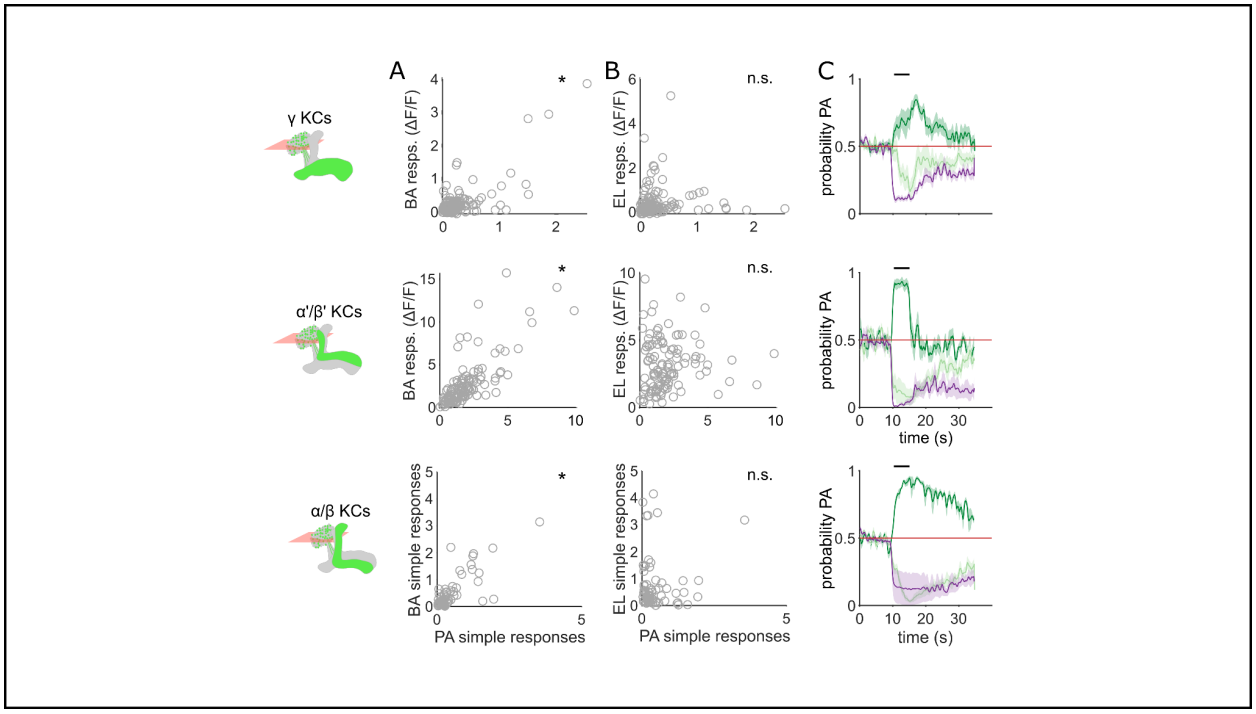

Similar odors have similar KC response patterns

A Scatter plots showing the similarity of the mean odor response of individual KCs to the two similar odors PA and BA. Correlations were significant across all three KC subtypes (γ KCs: Pearson's correlation coefficient, $r = 0.74$, $p < 0.001$; α'/β' KCs: $r = 0.76$, $p < 0.001$; α/β KCs: $r = 0.63$, $p < 0.001$).

B Scatter plots as in **A**, but for dissimilar odors PA and EL. No significant correlations in this case (γ KCs: $r = 0.044$, $p = 0.60$; α'/β' KCs: $r = 0.06$, $p = 0.55$; α/β KCs: $r = -0.04$, $p = 0.77$).

C Decoder-predicted probability that the odor delivered was PA, plotted against time. Prediction for trials on which PA was delivered are plotted in dark green, BA – light green and EL – purple. The red line indicates the positive prediction threshold. The black bar at the top indicates odor delivery period. Solid lines are mean, and shading indicates SEM. Probabilities are plotted for the same example fly as in Fig. 2 **C** for each KC type.

Figure 3:

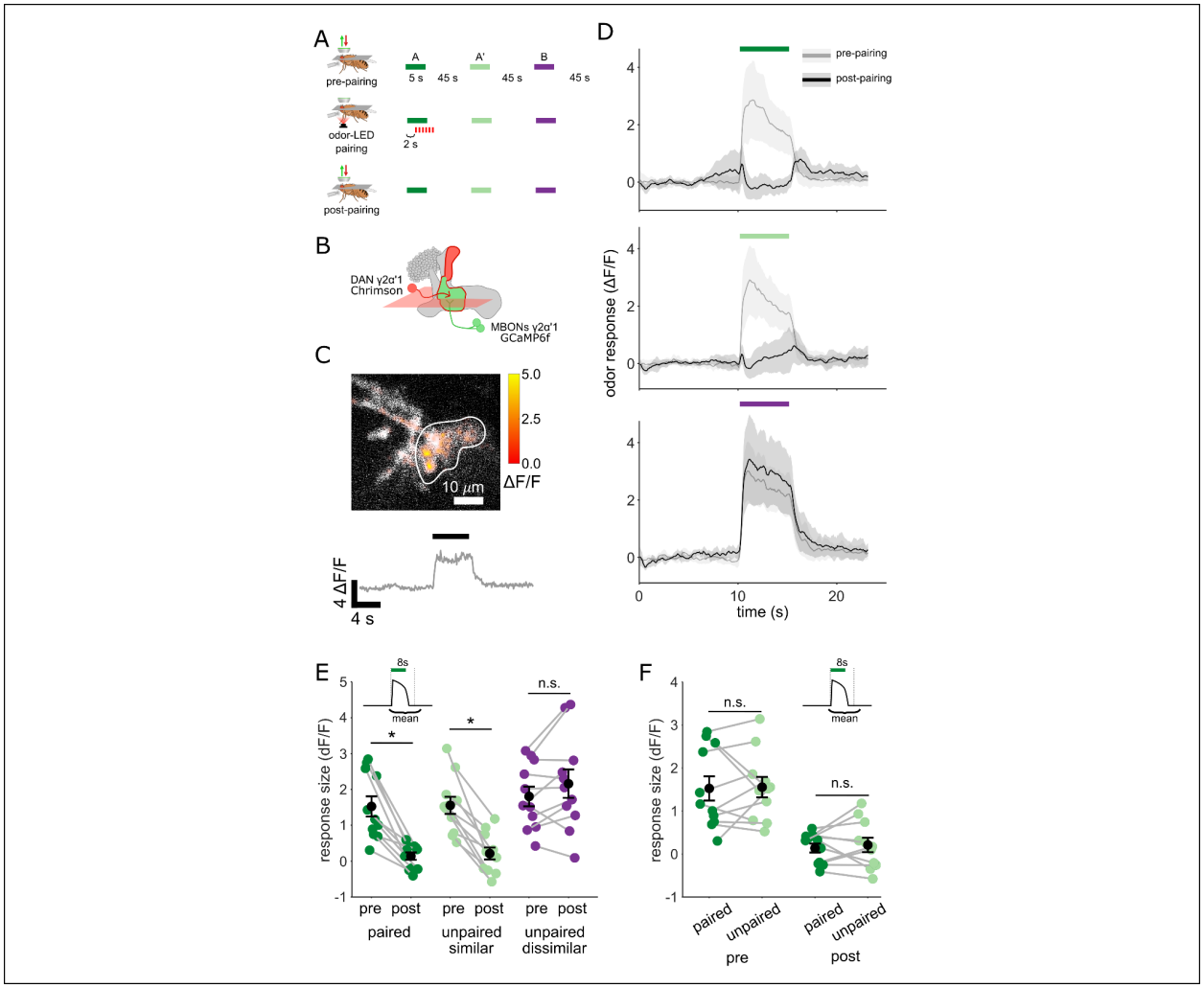

Plasticity in MBON γ2α'1 is not sufficiently odor specific for hard discrimination

A Stimulus protocol for on-rig, in vivo training. Plasticity in MBON γ2α'1 was assessed by imaging pre- and post-pairing with optogenetic reinforcement via DAN PPL1-γ2α'1. There was no imaging during the pairing itself. Colored bars represent 5s odor delivery (dark green: odor A paired; light green: odor A' unpaired similar; purple: odor B unpaired dissimilar). PA and BA were used as the paired odor for every alternate fly.

B Schematic of experimental design. Expression of GCaMP6f in MBON-γ2α'1 driven by MB077B-Gal4 and Chrimson88-tdTomato in DAN PPL1-γ2α'1 by 82C10-LexA. Imaging plane in the γ lobe as indicated.

C Example MBON-γ2α'1 single trial odor response. ΔF/F responses (color bar) are shown overlaid on baseline fluorescence (grayscale). White ROI indicates neuropil region for which a single-trial ΔF/F trace is plotted below. Black bar indicates odor delivery.

D MBON γ2α'1 ΔF/F response traces pre- (grey) and post- (black) pairing (mean +- SEM, n = 11 flies). Bars indicate 5s odor delivery period; colors correspond to odor identities in a.

E Response sizes pre- and post-pairing show a reduction for both paired (dark green, p = 0.001), and similar unpaired (light green, p = 0.001) odors but not the dissimilar odor (purple, p = 0.18). Response amplitude calculated as mean ΔF/F over an 8s window starting at odor onset (inset). Connected circles indicate data from individual flies.

F Data as in **E**, re-plotted to compare responses to the paired odor with responses to the unpaired, similar odor before and after training. Response sizes were not significantly different pre- ($p = 0.77$) or post-pairing ($p = 0.77$).

Statistical comparisons made with the paired sample Wilcoxon signed rank test, with a Bonferroni Holm correction for multiple comparisons.

Figure 4:

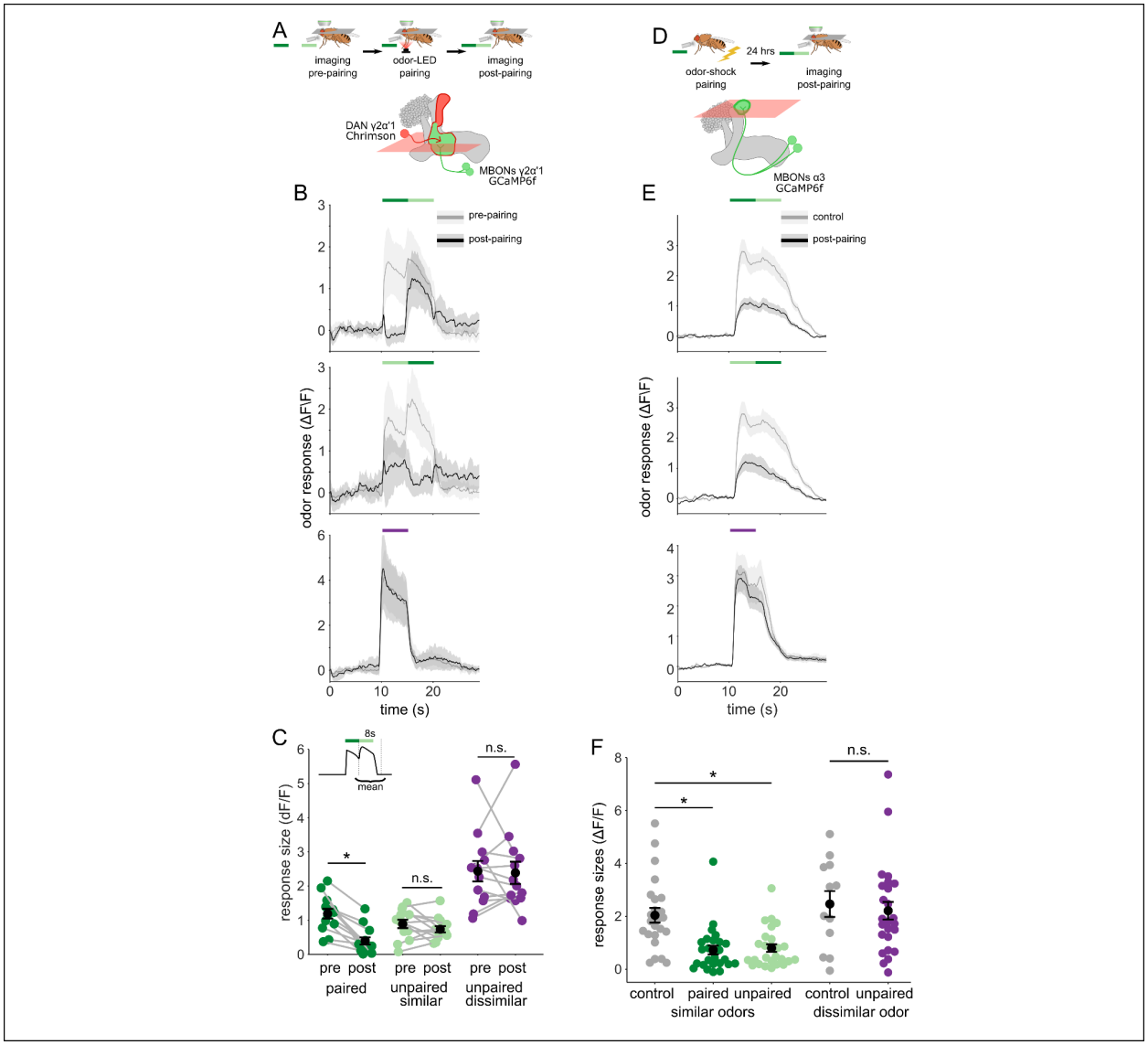

Odor transitions enable discrimination by MBON-γ2α'1 but not MBON-α3

A Schematic of experimental design to assess plasticity in MBON-γ2α'1. Protocol was identical to Fig. 3a, except odor transitions were used as pre- and post-pairing test stimuli to mimic odor boundaries from the behavioral arena. See Fig.4 Supplement 2a for the detailed protocol.

B MBON-γ2α'1 ΔF/F response time courses pre- (gray) and post- (black) pairing to different odor transitions (mean +- SEM, n = 13 flies). Colored bars indicate timing of odor delivery, dark green: paired odor, light green: unpaired, similar odor, purple: dissimilar odor. Schematic of the corresponding fly movement in the behavior arena at left.

C Response sizes in MBON-γ2α'1 pre- and post-pairing for the second odor in the transition. Responses calculated as mean over an 8s window starting at the onset of the second odor (inset). Responses when the paired odor is second are significantly reduced after pairing (dark green n = 13 flies, $p < 0.001$). By contrast there is no significant reduction when the unpaired similar odor comes second (light green $p = 0.376$). The dissimilar odor control showed no significant change (purple, $p=1$). Connected circles indicate data from individual flies.

D Schematic of experimental design for MBON-α3. Flies were trained by pairing odor with shock in a conditioning apparatus and odor responses were imaged 24 hours later. Plasticity was assessed by comparing responses against those from a control group of flies exposed to odor and shock but separated by 7 min. See Supplementary Fig. 34B for the detailed protocol. GCaMP6f was driven in MBON-α3 by MB082C-Gal4 (bottom).
E MBON-α3 ΔF/F response traces as in **B**. Light gray traces are from control shock-exposed flies (n = 12 flies), dark gray traces are from odor-shock paired flies (pooled n = 14 PA-paired and n = 12 BA-paired flies). Averaged control traces were pooled across trials where either PA or BA was the second odor in a transition.
F Response sizes in MBON-α3 in control (gray) and trained flies (colored) for the second odor in the transition (computed as in **C**). Responses are significantly reduced in trained flies both when the paired odor is second (dark green, n = 14 PA-paired and n = 12 BA-paired flies pooled, $p < 0.001$) and when the unpaired similar odor is second (light green, $p < 0.001$). Responses to the dissimilar odor were not significantly different (purple, $p = 0.48$). Plotted control responses were pooled across trials where PA or BA was the second odor in a transition.
C, F Statistical comparisons for MBON-γ2α'1 made with the paired sample, Wilcoxon signed-rank test. For MBON-α3, where responses were compared across different flies, we used the independent samples Wilcoxon's rank-sum test. p-values were Bonferroni-Holm corrected for multiple comparisons.

Supplementary figure 2:

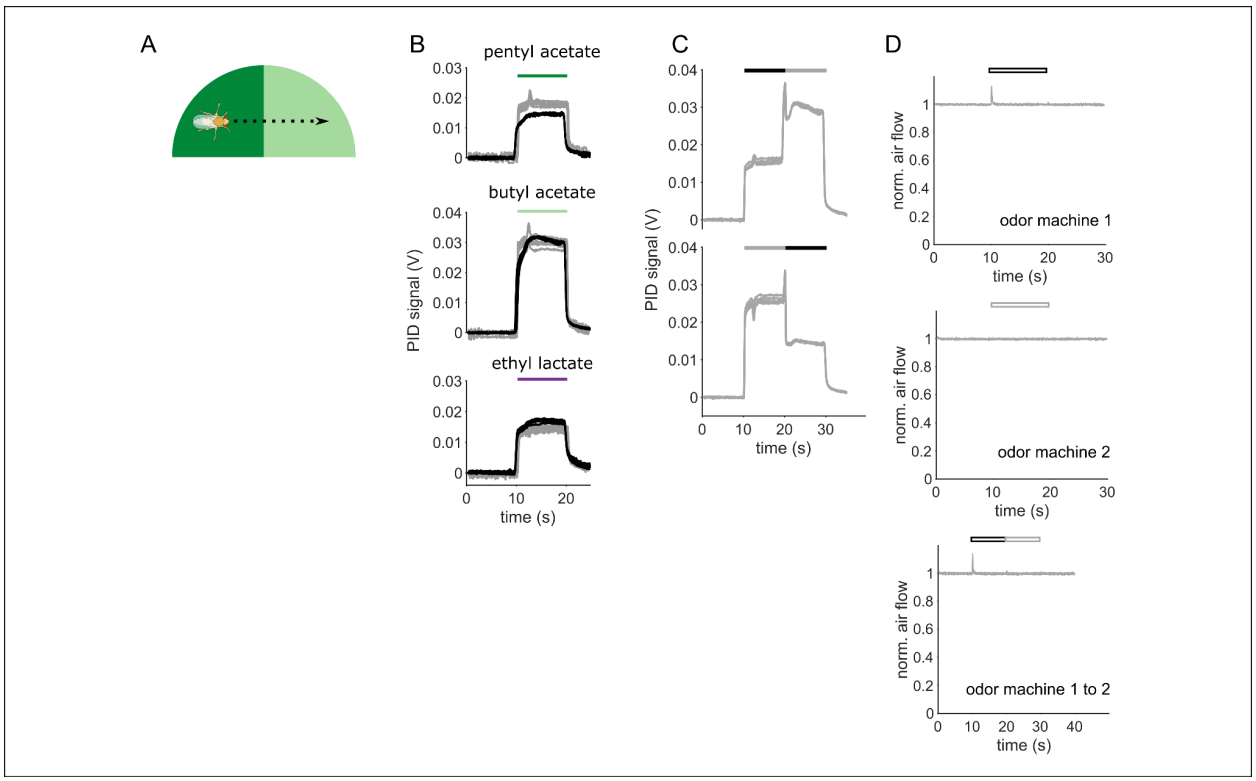

Time courses of odor delivery and air flow for odor pulses and odor transitions
A Schematic showing a fly crossing a boundary between the paired and unpaired odor quadrants in the behavior arena. As the fly crosses the boundary, it experiences odors as a transition in time.
B Photo-ionization detector (PID) signals for the odor stimuli used in this study. Single odor pulses from odor machine 1 shown in black (traces for five repeats overlaid) and pulses from odor machine 2 in gray.

Note that at a given concentration in air, each odor-chemical can generate different ionization signal amplitudes.

C PID traces for odor transitions PA to BA (top) and BA to PA (bottom). Throughout this study, the first odor pulse was always delivered by odor machine 1 and the second pulse by machine 2.

D Hot-wire anemometer measurements of change in air velocity relative to steady-state flow. Top two panels are single stimulus pulses from each odor machine, bottom is for a transition stimulus. Hollow bars indicate that these measurements were taken without odorants in the airflow to avoid chemical interactions with the anemometer. Steady state flow rate as measured with a floating-ball flowmeter was 400 mL/min.

Supplementary figure 3:

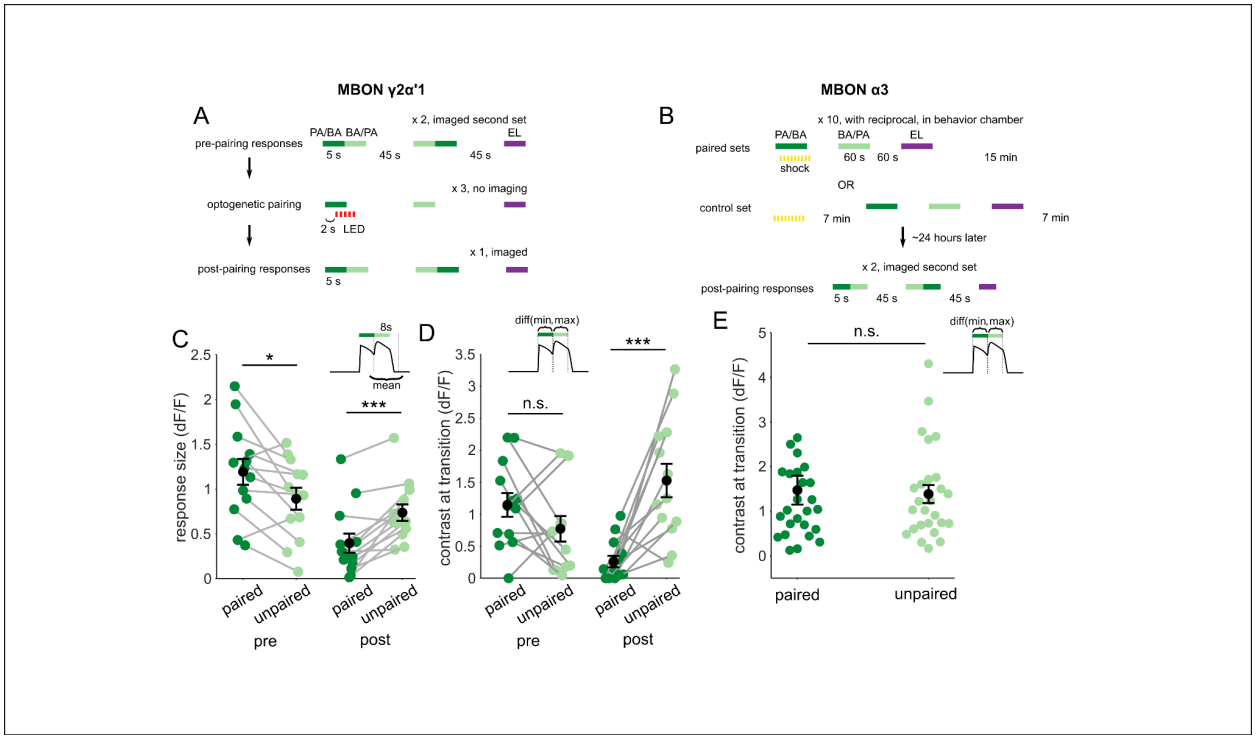

Contrast around odor transitions is high for MBON-γ2α'1 but not MBON-α3

A, B Detailed schematics for training protocols used in Fig 4.

A For MBON-γ2α'1, we imaged pre- and post-pairing responses to 5s pulses of the two similar odors presented as transitions, and the dissimilar odor presented singly. Each pairing trial consisted of a single 5 s odor stimulus paired with 5s of LED flashes, followed by 5s presentations of the similar unpaired odor and the dissimilar odor, with 45s in between each odor presentation. Pairing was repeated three times with 45s between pairing trials. Each of the similar odors was paired with LED reinforcement for every alternate imaged fly as part of a reciprocal experiment design.

B For MBON-α3, we only imaged post-pairing responses, 24 hours after odor-shock reinforcement. This is because learning is only expressed hours after reinforcement in this compartment. A pairing trial consisted of a single, 60s odor presentation paired with shock, followed by 60s presentations of the unpaired similar and dissimilar odors, with 60s in between each odor presentation. Pairing was repeated 10 times, with 15 min between pairing trials. PA and BA were used as the paired odor alternate sets of flies as odor reciprocals. We could not measure the odor responses of flies before learning. So, we

measured un-paired odor responses in flies that were exposed to shock and odor stimuli of equal durations, except with a 7 min interval between shock and the first odor stimulus in mock-pairing trials. These were the shock-exposed controls.

C Same data as Fig. 4c, quantifying responses to the second odor pulse, but re-plotted to compare responses to the paired odor with responses to the unpaired, similar odor before and after training. Pre-pairing, the responses to the paired odor were slightly but significantly higher ($p = 0.02$), but post-pairing, responses to the unpaired similar odor were higher ($p = 0.004$).

D Contrast scores at the different odor transitions for MBON-γ2α'1 responses. Labels indicate the odor coming second in the transition. Contrast calculated as the difference between the maximum $\Delta F/F$ value during the second pulse and the minimum during the first pulse (inset). Pre-pairing, contrast was not different for the two kinds of transitions ($p = 0.19$). Post-pairing contrast was higher for the transition to the unpaired, similar odor ($p = 0.001$). Connected circles indicate data from individual flies. Statistical comparisons made using the paired sample Wilcoxon signed rank test with a Bonferroni Holm correction for multiple comparisons.

E Contrast scores as d, for MBON-α3 responses in arena-trained flies. Contrast scores were not significantly different for the two directions of the transition ($n = 14$ PA-paired and 12 BA-paired flies, pooled, $p = 0.86$). Statistical comparison made with independent sample Wilcoxon's rank-sum test, with Bonferroni-Holm corrections for multiple comparisons.

Supplementary figure 4:

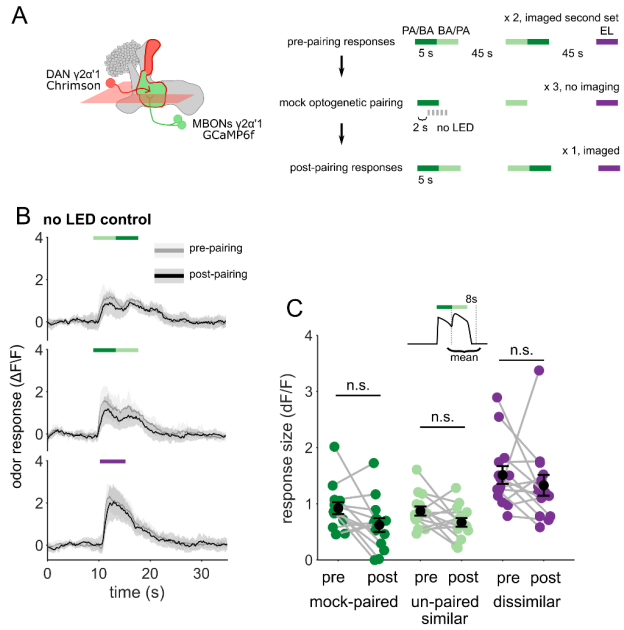

No plasticity in MBON-γ2α'1 with no-LED control training protocol

A Protocol schematic. Same as in Supplementary Fig. 4A, except with no LED flashes in the training trials.

B MBON-γ2α'1 ΔF/F response time courses to different odor transitions pre- (gray) and post- (black) no-LED control training (mean +- SEM, n = 14 flies). Colored bars indicate timing of odor delivery, dark green: paired odor, light green: unpaired similar odor, purple: dissimilar odor.

C Response sizes in MBON-γ2α'1 for the second odor in the transition with no-LED control training protocol. Response amplitude calculated as mean over an 8s window starting at the onset of the second odor (inset). Responses are not significantly reduced for any stimulus (n=14 flies; paired odor: p = 0.06; unpaired, similar odor p = 0.17; dissimilar odor p = 0.19).

Figure 5

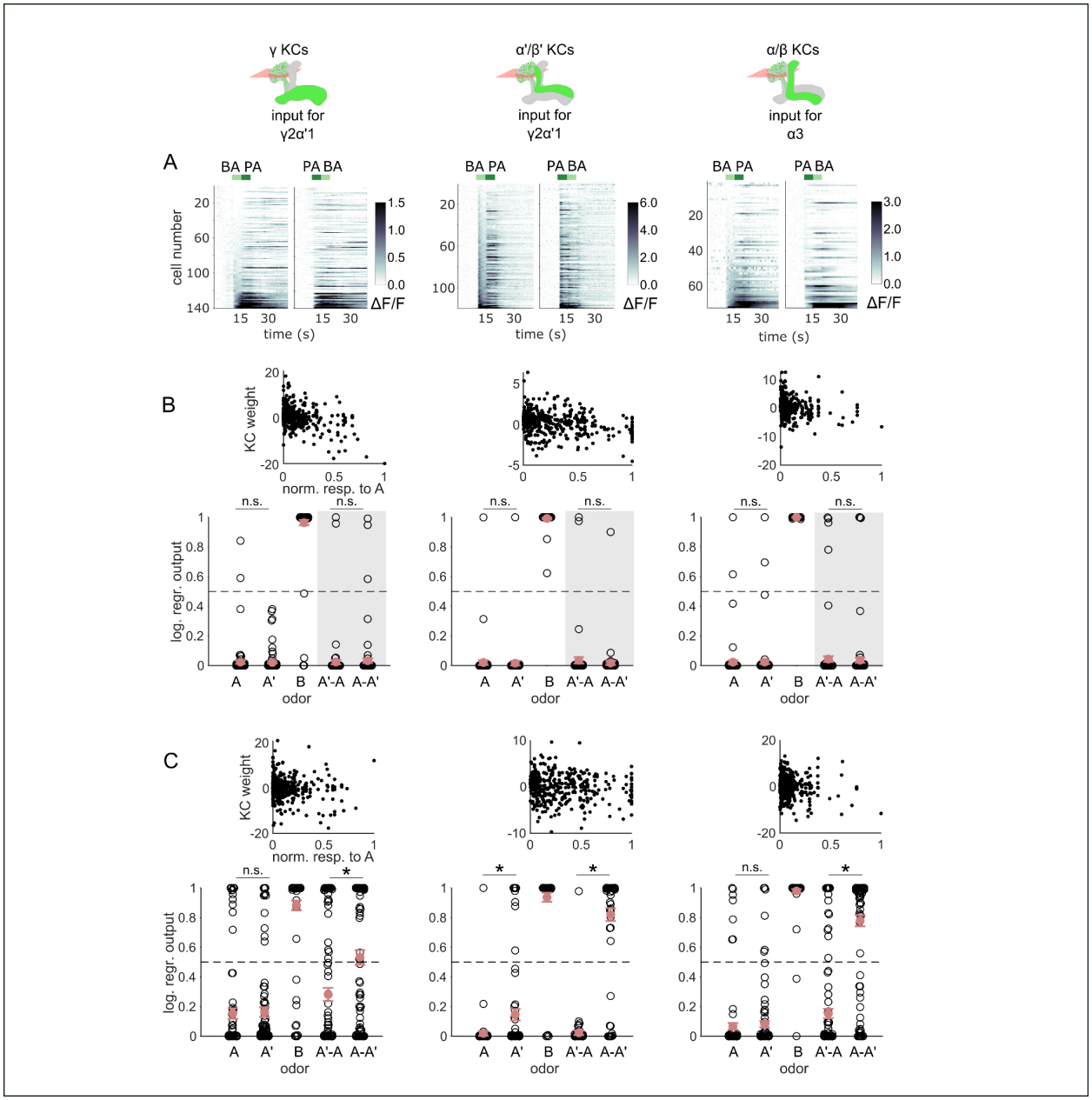

KC responses to odor transitions and a simple learning rule are not sufficient for hard discrimination

A ΔF/F responses of different KC subtypes to odor transitions. Rows show responses of individual KCs, averaged across trials, sorted by responses to BA-PA. GCaMP6f was driven in γ KCs by d5HT1b-Gal4 (left), in α'/β' KCs by c305a-Gal4 (middle) and in α/β KCs by c739-Gal4 (right). The odor delivery periods are indicated by colored bars at the top.

B We fitted KC weights with logistic regression to give high or low outputs to odors consistent with measured MBON outputs (synaptic weight plots, black circles are individual fitted weights, pooled across flies). Individual logistic regression model outputs for held out test data for all types of odor stimuli are plotted in black. Outputs with a gray background are for stimuli not part of the training set (n = 96 models

for γ, n = 80 for α'/β' and n = 96 for α/β KCs respectively), red circles and error bars are mean +/- SEM. The dashed, gray line at 0.5 indicates the logistic regression output threshold. Mean model outputs were below the decision threshold for A and A' and were not significantly different ($p = 1$ for γ, $p = 1$ for α'/β' and $p = 1$ for α/β KCs respectively), as was the case for A'-A and A-A' ($p = 1$ for γ, $p = 1$ for α'/β' and $p = 1$ for α/β KCs respectively).

C Fitted weights and outputs for logistic regression models as in B, except that these were trained on single pulse as well as odor transitions. Average model outputs for A and A' were below the decision threshold and were significantly different only for one KC sub-type ($p = 0.022$ for γ, $p < 0.001$ for α'/β' and $p = 0.048$ for α/β KCs respectively). Mean outputs for A'-A were below the decision threshold, but outputs for A-A' were above it and significantly different for all KC subtypes ($p < 0.001$ for γ, $p < 0.001$ for α'/β' and $p < 0.001$ for α/β KCs respectively).

All statistical comparisons were made with the Wilcoxon signed-rank test with a Bonferroni-Holm correction for multiple comparisons.

Figure 6:

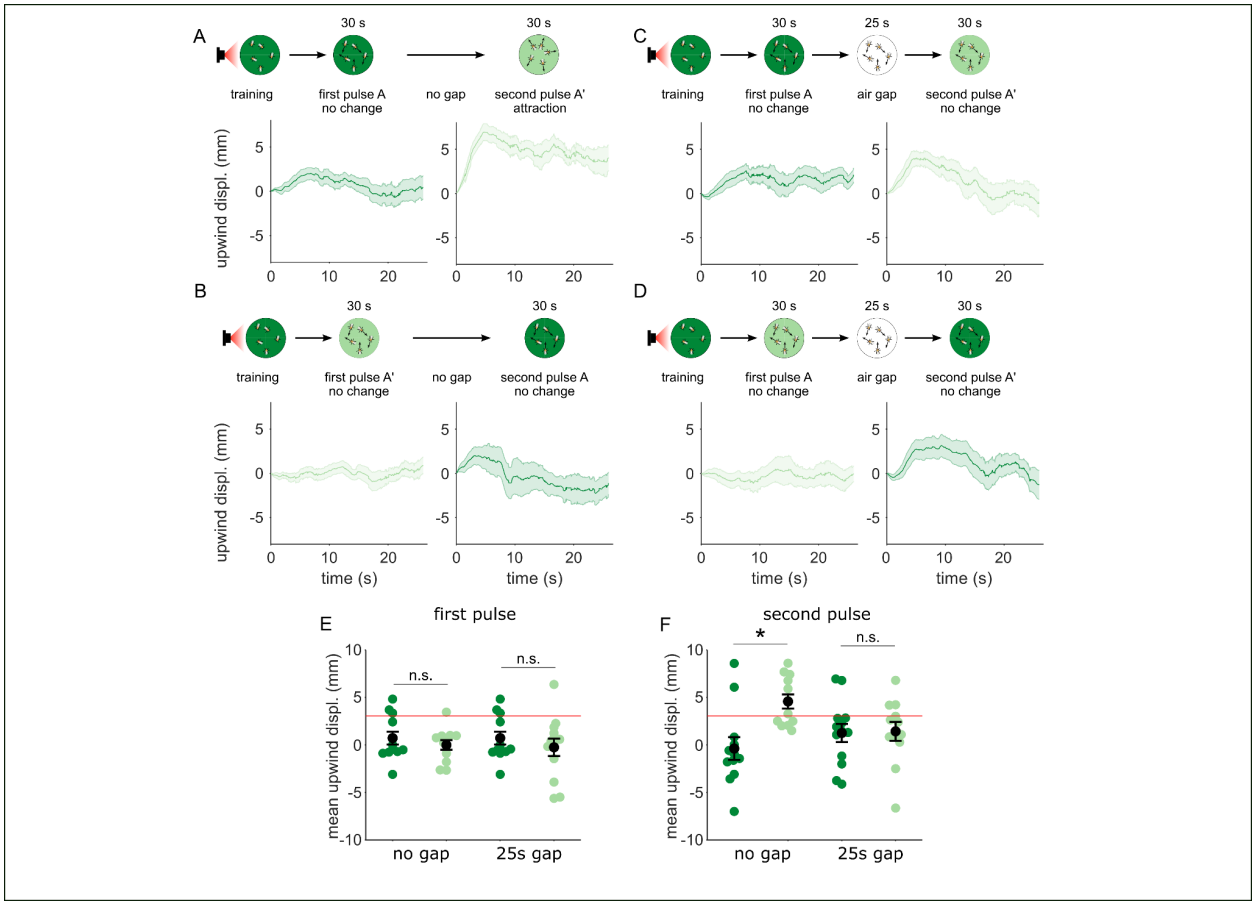

Flies are attracted to the unpaired odor only in transitions

A-D, top: Schematic of experiment strategy to measure behavioral response to odor transitions. Flies were trained by pairing one of the similar odors with optogenetic activation of γ2α'1 DANs. They were then presented 30s odor pulses, either as transitions in time (A, B), or transitions interrupted by a 25s air period (C, D).

A Upwind displacement in the first and second pulses of an A-A' odor transition, as indicated by the schematics above each panel. This was computed as the increase in each fly's distance from the arena center over the odor delivery period, then averaged across all flies in an arena (approximately 15 flies per arena). Traces in dark and light green are responses to A and A' respectively. Plots are mean +/- SEM (n = 12 arena runs for all stimulus types).

B Upwind displacement for the reversed odor transition ie. A'-A.

C Upwind displacement for A - air - A' interrupted transition.

D Upwind displacement for the reversed, A' - air - A interrupted transition.

E Upwind displacement in response to the first odor pulse, averaged across flies in each arena experiment. Mean displacement was not significantly different between unpaired and paired odors for experiments with no gap (n = 12, 12 experiments for paired and unpaired odors, p = 0.70) and a 25 s gap (n = 12, 13, p = 0.40). The red line represents the mean upwind displacement in response to direct, optogenetic activation of MBON-γ2α'1.

F As in **E** except for responses to the second odor pulse. Displacement was significantly different for transitions with no gap between pulses (n = 12, 12 experiments for paired and unpaired odors, p = 0.004) but not different when transitions were interrupted by a 25s gap (n = 12, 13, p = 0.85).

Statistical comparisons in **E** and **F** were made with the independent-sample Wilcoxon rank sum test with a Bonferroni Holm correction for multiple comparisons.

Supplementary figure 6:

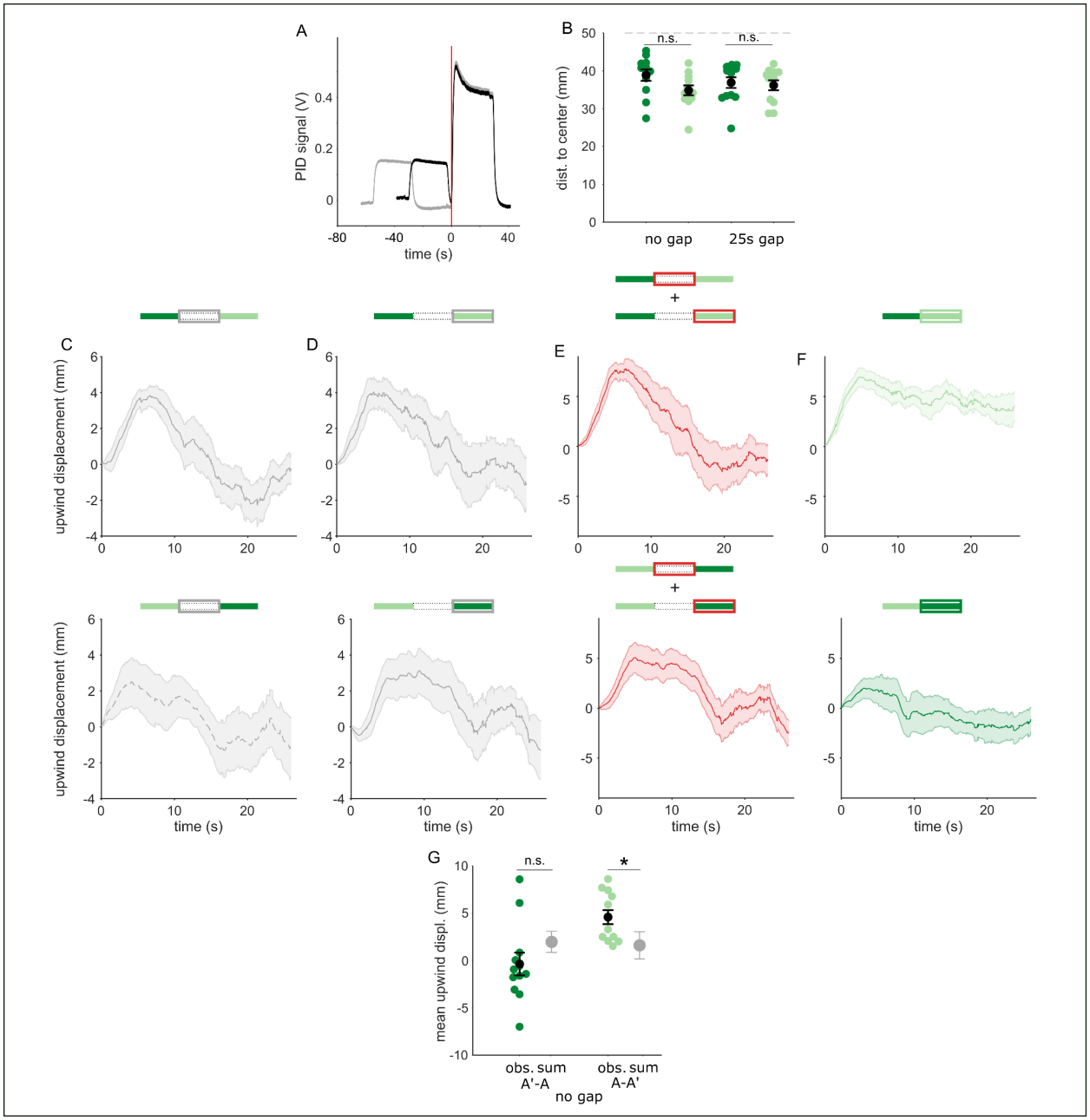

Transition dependent attraction is not a result of linearly summed, single-pulse responses

A PID measurements of odor time courses in the behavioral arena, measured at the central exhaust port. The black trace depicts odor pulses delivered with no gap and the gray trace depicts pulses interrupted by a 25s air period. The vertical red line indicates the time point identified as the onset of the second odor pulse.

B Mean distances of flies from the arena center at the onset of the second odor pulse in each experiment. Distances from the center were not significantly different between experiments with the unpaired and paired odor, with a 0s gap (n = 12, 12 resp. p = 0.08) or with a 25s gap (n = 12, 13, p = 0.39). Statistical comparisons made with the independent samples, Wilcoxon's rank sum test followed by a Bonferroni-Holm correction for multiple comparisons.

C The off response trace after the first odor pulse for A-A' transitions without an air gap (top) and A'-A transitions with an air gap (bottom).
D The response at the onset of the second odor pulse for A-A' transitions without an air-gap (top) and A'-A transitions with an air gap (bottom).
E The linear sum of upwind displacement traces in C and D. This is the null model to compare with responses to an odor transition.
F Actual displacement during the second odor pulse in unpaired to paired transition stimuli with no air-gap. Traces in C-F are mean +/- SEM.
G Mean upwind displacement over the duration of the second odor pulse for the two transitions (dark green: A' to A, light green; A to A'). In gray is the mean and bootstrapped SEM of the linear sum of component responses in C. The measured displacements are significantly greater than the sum when odor A' is second ($n=12$, $p = 0.001$) but not when odor A is second ($n=12$, $p = 0.09$). Displacements were compared with the Wilcoxon's signed rank test followed by a Bonferroni-Holm correction for multiple comparisons.